CENTRAL RESEARCH LIBRARY
DOCUMENT COLLECTION

[redacted]

ORNL-2052
Progress cy. 95-A
C-84 – Reactors–Special Features of Aircraft Reactors

AEC RESEARCH AND DEVELOPMENT REPORT

MARTIN MARIETTA ENERGY SYSTEMS LIBRARIES
3 4456 0350105 7

DECLASSIFIED
CLASSIFICATION CHANGED TO:
BY AUTHORITY OF: AEC 7-12-60
BY: Bowman 3/26/60

SOLID STATE DIVISION

SEMIANNUAL PROGRESS REPORT

FOR PERIOD ENDING FEBRUARY 29, 1956

CENTRAL RESEARCH LIBRARY
DOCUMENT COLLECTION
LIBRARY LOAN COPY
DO NOT TRANSFER TO ANOTHER PERSON
If you wish someone else to see this document, send in name with document and the library will arrange a loan.

OAK RIDGE NATIONAL LABORATORY
OPERATED BY
UNION CARBIDE NUCLEAR COMPANY
A Division of Union Carbide and Carbon Corporation
UCC
POST OFFICE BOX P · OAK RIDGE, TENNESSEE

[redacted]

LEGAL NOTICE

This report was prepared as an account of Government sponsored work. Neither the United States, nor the Commission, nor any person acting on behalf of the Commission:

A. Makes any warranty or representation, express or implied, with respect to the accuracy, completeness, or usefulness of the information contained in this report, or that the use of any information, apparatus, method, or process disclosed in this report may not infringe privately owned rights; or

B. Assumes any liabilities with respect to the use of, or for damages resulting from the use of any information, apparatus, method, or process disclosed in this report.

As used in the above, "person acting on behalf of the Commission" includes any employee or contractor of the Commission to the extent that such employee or contractor prepares, handles or distributes, or provides access to, any information pursuant to his employment or contract with the Commission.

[redacted]

ORNL-2052
Progress
C-84 – Reactors–Special Features of Aircraft Reactors

This document consists of 48 pages.
Copy 95 of 298 copies. Series A.

Contract No. W-7405-eng-26

SOLID STATE DIVISION

SEMIANNUAL PROGRESS REPORT

For Period Ending February 29, 1956

D. S. Billington, Director
J. H. Crawford, Jr., Assistant Director

DATE ISSUED

JUN 12 1956

OAK RIDGE NATIONAL LABORATORY
Operated by
UNION CARBIDE NUCLEAR COMPANY
A Division of Union Carbide and Carbon Corporation
Post Office Box P
Oak Ridge, Tennessee

[redacted]

MARTIN MARIETTA ENERGY SYSTEMS LIBRARIES
3 4456 0350105 7

[redacted]

Reports previously issued in this series are:

ORNL-1025	Period Ending January 31, 1951
ORNL-1095	Period Ending April 30, 1951
ORNL-1128	Period Ending July 31, 1951
ORNL-1214	Period Ending October 31, 1951
ORNL-1261	Period Ending January 31, 1952
ORNL-1301	Period Ending May 10, 1952
ORNL-1359	Period Ending August 10, 1952
ORNL-1429	Period Ending November 10, 1952
ORNL-1506	Period Ending February 10, 1953
ORNL-1606	Period Ending August 31, 1953
ORNL-1677	Period Ending February 28, 1954
ORNL-1762	Period Ending August 30, 1954
ORNL-1851	Period Ending February 28, 1955
ORNL-1944	Period Ending August 30, 1955
ORNL-1945	Period Ending August 30, 1955
ORNL-2051	Period Ending February 29, 1956

[redacted]

[redacted]

INTERNAL DISTRIBUTION

1. C. D. Baumann
2. R. G. Bergren
3. J. O. Betterton, Jr.
4. D. S. Billington
5. D. Binder
6. T. H. Blewitt
7. A. L. Boch
8. C. D. Bopp
9. B. S. Borie
10. G. E. Boyd
11. E. J. Boyle
12. H. Brooks (consultant)
13. W. E. Browning
14. W. E. Brundage
15. D. W. Cardwell
16. R. M. Carroll
17. C. E. Center
18. R. A. Charpie
19. J. W. Cleland
20. G. H. Clewett
21. A. F. Cohen
22. D. D. Cowen
23. J. H. Crawford, Jr.
24. F. L. Culler
25. J. E. Cunningham
26. R. R. Dickison
27. S. E. Dismuke
28. L. B. Emlet (K-25)
29. M. J. Feldman
30. J. H. Frye, Jr.
31. J. L. Gabbard
32. R. J. Gray
33. W. O. Harms (consultant)
34. C. S. Harrill
35. A. Hollaender
36. D. K. Holmes
37. A. S. Householder
38. J. T. Howe
39. L. K. Jetter
40. R. W. Johnson
41. R. J. Jones
42. W. H. Jordan
43. G. W. Keilholtz
44. C. P. Keim
45. M. T. Kelley
46. R. H. Kernohan
47. E. M. King
48. H. V. Klaus
49. G. E. Klein
50. T. A. Lincoln
51. S. C. Lind
52. R. S. Livingston
53. H. G. MacPherson (consultant)
54. W. D. Manly
55. E. J. McHargue
56. A. J. Miller
57. E. C. Miller
58. J. G. Morgan
59. K. Z. Morgan
60. E. J. Murphy
61. J. P. Murray (Y-12)
62. M. L. Nelson
63. R. B. Oliver
64. W. W. Parkinson
65. P. M. Reyling
66. M. T. Robinson
67. E. S. Schwartz
68. H. C. Schweinler
69. F. Seitz (consultant)
70. E. D. Shipley
71. O. Sisman
72. M. J. Skinner
73. G. P. Smith
74. A. H. Snell
75. R. L. Sproull (consultant)
76. E. E. Stansbury
77. D. K. Stevens
78. W. J. Sturm
79. C. D. Susano
80. J. A. Swartout
81. E. H. Taylor
82. J. M. Warde
83. C. C. Webster
84. M. S. Wechsler
85. R. A. Weeks
86. A. M. Weinberg
87. E. P. Wigner (consultant)
88. G. C. Williams
89. W. R. Willis
90. J. C. Wilson
91. C. E. Winters
92. M. C. Wittels

[redacted]

[redacted]

93. Biology Library
94-96. Central Research Library
97. Health Physics Library
98-102. Laboratory Records Department
103. Laboratory Records, ORNL R. C.
104. ORNL – Y-12 Technical Library, Document Reference Section
105. Reactor Experimental Engineering Library

EXTERNAL DISTRIBUTION

106. AF Plant Representative, Baltimore
107. AF Plant Representative, Burbank
108. AF Plant Representative, Marietta
109. AF Plant Representative, Santa Monica
110. AF Plant Representative, Seattle
111. AF Plant Representative, Wood-Ridge
112. Air Materiel Area
113. Air Research and Development Command (RDGN)
114. Air Research and Development Command (RDZPA)
115. Air Technical Intelligence Center
116. Aircraft Laboratory, Design Branch (WADC)
117-119. ANP Project Office, Fort Worth
120. Argonne National Laboratory
121. Armed Forces Special Weapons Project, Sandia
122. Assistant Secretary of the Air Force, R&D
123-128. Atomic Energy Commission, Washington
129. Battelle Memorial Institute
130. Bettis Plant
131. Bureau of Aeronautics
132. Bureau of Aeronautics (Code 24)
133. Bureau of Aeronautics General Representative
134. Chicago Operations Office
135. Chicago Patent Group
136-137. Chief of Naval Research
138. Convair, General Dynamics Corporation
139. Director of Laboratories (WCL)
140. Director of Requirements (AFDRQ)
141. Director of Research and Development (AFDRD-ANP)
142-144. Directorate of Systems Management (RDZ-1SN)
145-147. Directorate of Systems Management (RDZ-1SS)
148. Equipment Laboratory (WADC)
149-152. General Electric Company (ANPD)
153. Hartford Area Office
154. Headquarters, Air Force Special Weapons Center
155. Idaho Operations Office
156. Knolls Atomic Power Laboratory
157. Rockland Area Office
158. Los Alamos Scientific Laboratory
159. Materials Laboratory Plans Office (WADC)
160. National Advisory Committee for Aeronautics, Cleveland
161. National Advisory Committee for Aeronautics, Washington
162. Naval Air Development Center
163. New York Operations Office
164. North American Aviation, Inc. (Aerophysics Division)

[redacted]

[redacted]

165. Nuclear Development Corporation
166. Patent Branch, Washington
167-169. Powerplant Laboratory (WADC)
170-173. Pratt and Whitney Aircraft Division (Fox Project)
174. San Francisco Operations Office
175. Sandia Corporation
176. School of Aviation Medicine
177. Sylvania Electric Products, Inc.
178. USAF Project RAND
179. University of California Radiation Laboratory, Livermore
180-182. Wright Air Development Center (WCOSI-3)
183-298. Technical Information Extension, Oak Ridge
299. Division of Research and Development, AEC, ORO

[redacted]

[redacted]

CONTENTS

SUMMARY 1

REVIEW OF CORROSION AND FUEL STABILITY UNDER IRRADIATION 3

Capsule Tests (In-Pile) 3

Forced-Flow Loops (In-Pile) 3

Results from In-Pile Loops 3

RADIATION METALLURGY 5

Stress Corrosion 5

Alternate Stress-Corrosion Experiment 7

MTR Tensile Creep 8

Pneumatic Stressing Device 9

Ductility of Nickel Alloys 9

ENGINEERING PROPERTIES 11

Radiation Damage to Ceramic Fuel Materials 11

Furnace and Calorimeter for Remote Determination of Specific Heat 12

Radiation Damage to Boron Carbide 14

REACTOR EXPERIMENTS 20

Effect of Radiation on Static Corrosion by Fused Salt 20

Holdup of Fission Gases by Charcoal Traps 20

LITR Vertical Loop 24

ART Off-Gas Analysis 25

Flux Measurements 25

Inconel as a Thermal-Flux Monitor 25

Fast-Flux Measurements 27

CHEMICAL EFFECTS OF NUCLEAR REACTIONS 28

Effects of the Fission Products on the Properties of ANP Fluoride Fuels 28

Use of Natural Lithium in In-Pile Corrosion Testing of ANP Fluoride Fuels 31

SPECIAL PROJECTS 33

Hot Metallography 33

Hot-Cell Operation 39

[redacted]

[redacted]

SOLID STATE DIVISION SEMIANNUAL PROGRESS REPORT

SUMMARY

REVIEW OF CORROSION AND FUEL STABILITY UNDER IRRADIATION

The fluoride fuels have retained their stability under irradiation. Corrosion data are about the same for irradiated and unirradiated Inconel capsules containing the fused salts. Three in-reactor loops have shown low corrosion results, as indicated by metallographic examination, and the results are confirmed by chemical analysis of the fuel.

RADIATION METALLURGY

Eight stress-rupture tests at a stress of 2000 psi, in helium, have been completed in the LITR. Bench-test data for comparison is not yet available.

Metallographic examination of at least 25 thin-wall Inconel specimens that gave indications of defects in eddy-current and ultrasonic inspections by the Metallurgy Division disclosed only one visibly flawed tube.

Flux measurements in hole HB-3 of the LITR have shown that a thermal flux of 9×10^{12} neutrons $\cdot$ cm$^{-2} \cdot$ sec^{-1} is available at the surface of a mockup capsule with a cross section equivalent to that of fuel salts. Flux attenuation through the mockup fuel was also measured.

Tubular Inconel creep specimens subjected to a tensile stress of 1500 psi at 1500°F, in helium, for 33 days in hole HB-3 of the MTR were found to have fractured. Postirradiation examination has suggested that localized high temperatures or an unidentified film caused premature fracture.

Elevated-temperature tensile tests on monel, Inconel, and Nichrome have so far shown that the ductility minimum found at about 1000°F is strain-rate dependent. A ductility minimum is not found in monel at low testing speeds.

ENGINEERING PROPERTIES

Radiation Damage to Ceramic Fuel Materials. – A new program has been initiated to study the radiation stability of ceramic fuels at elevated temperatures. Two materials are receiving first consideration: ThO_2-UO_2 and SiC-Si-UO_2. An irradiation is in progress in which an SiC-Si-UO_2 specimen is held at 1750°F, in a closed container of helium, by its own fission heat. A heat-capacity apparatus has been built and calibrated. Other important tests will include: determinations of strength, elastic properties, fission-gas release, and dimensional changes; x-ray diffraction; and microscopic examination.

Radiation Damage to Boron Carbide. – Specimens of hot-pressed and cold-pressed sintered B_4C were irradiated in the LITR for six weeks. They were sealed in quartz ampoules in a helium atmosphere and placed directly in the reactor water in hole C-48. No gas pressure and no loss in weight or change in physical appearance were found in the hot-pressed material. The cold-pressed sintered material left a black deposit on the ampoule, and pressure in the ampoule indicated decomposition of some foreign material in the B_4C. Further tests are in progress, and more irradiations are planned for coated specimens.

REACTOR EXPERIMENTS

Seven additional Inconel capsules containing fused-salt fuels have been irradiated in the MTR for periods of six to nine weeks and are being sampled. Facilities have been put into service for irradiating two or three capsules simultaneously in a hitherto unused high-flux position in the MTR.

The holdup behavior of radiokrypton in charcoal traps saturated with nitrogen or with helium was investigated over the temperature range −110 to +25°C. A theoretical expression was developed which was fitted to the results and may be used for the prediction of other conditions or for optimum design of traps to be used for retention of fission gases or for other purposes.

The second LITR vertical loop for circulating fused salt was prepared for insertion in the reactor.

Design conditions for the gamma spectrometer for the off-gas system of the ART were established.

A flux monitoring system using Inconel has been developed for use at high temperatures. Chromium-51 activity is followed for exposure times up to one or two months. The $Co^{59}(n,\gamma)Co^{60}$ reaction

[redacted]

in the Inconel is used for longer exposures. Flux measurements were made for the first LITR vertical loop and for the MTR loop operated by the Aircraft Reactor Engineering Division. Fast-flux profiles were obtained for hole 19 in the ORNL Graphite Reactor.

CHEMICAL EFFECTS OF NUCLEAR REACTIONS

Effects of the Fission Products on the Properties of ANP Fluoride Fuels. – Although theoretical considerations predict a substantial increase in the corrosion of Inconel by fused fluoride fuels under irradiation, this has never been observed experimentally. The deposit of the fission-product metals, ruthenium, niobium, and (presumably) molybdenum, appears to inhibit attack of the fuel on the container surface. The excess oxidizing power of the irradiated fuel, due to imbalance of fluorine between UF_4 and the fission-product fluoride mixture, is thus prevented from increasing corrosion.

Use of Natural Lithium in In-Pile Corrosion Testing of ANP Fluoride Fuels. – The tritium produced by the $Li^6(n,t)He^4$ reaction is expected to cause a large increase in the corrosion of metal capsules by fuels in the NaF-KF-LiF-UF_4 system. In order to prevent this, not more than 0.2% of the lithium can be present as Li^6. In in-pile loops, up to 1% Li^6 can be permitted without depressing the neutron flux unduly and without causing serious increases in corrosion.

SPECIAL PROJECTS

Hot Metallography. – Metallographic examination of GE-ANP-3E and GE-ANP-3W fuel plates revealed that failure of the 3E plate was a result of improper thermocouple placement, which caused localized overheating. Failure of the 3W fuel plate was thought to be caused by failure of the cladding as a result of fission-gas blister formation.

Work has continued on examination of specimens from the Homogeneous Reactor Project. Reports covering the results are awaiting examination of other specimens from each experiment.

Examination of sections from the North Carolina State University Reactor has begun; sections from the core tank have shown only light corrosive attack, with the exception of an area near the liquid-vapor interface, where complete penetration was observed. Evidence of stress-corrosion attack was noted at the interior surfaces of the cooling-coil tubing. Results will be published after examination of other samples are completed.

Disassembly of the ANP fuel loop No. 3 has begun. Metallographic specimens from the nose coil and a large portion of the fuel lines have been examined. Examination of these sections in the as-polished condition revealed no evidence of corrosive attack. In the etched condition, what appears to be moderately intergranular attack of approximately 1 mil in depth is apparent. This may be only an etching effect, however, since considerable difficulty has been encountered in the etching of these samples. Sectioning of the pump and the remaining lengths of fuel tubing, and chemical analysis of both the fuel and fuel tubing will begin shortly. Provisions for the disassembly of the next loop are being made.

Examination of four pin-type fuel elements irradiated by KAPL revealed fracture of the cladding where the core of the element made its closest approach to the exterior surface. No corrosive attack upon the clad was noted. A distinct change in the UO_2 particles was observed in comparing the irradiated and the nonirradiated control samples.

Examination of the final two P&W-ORNL-BMI fuel-element capsules has been finished. Blistering was noted in plates of both the small ($<3\ \mu$) and the larger ($15–44\ \mu$) UO_2 particle sizes. Since time was the only variable which had not been exceeded in previous experiments, it appears that time must now be added to temperature and burnup as variables in the study of the factors resulting in blistering of fuel elements.

Hot-Cell Operation. – HRP in-pile loop L-4-8 and the vertical dynamic-corrosion loop were disassembled in the hot cells. Impact and tensile measurements on various metals were carried out for both the ANP and the HRP. Work was completed on the last two Pratt & Whitney Aircraft solid fuel-element capsules (PW-1-12 and PW-1-13). New hot-cell equipment installed in the last period included a General Mills manipulator and an in-cell shielded storage facility. Data concerning use of the hot cells for the calendar year 1955 were correlated.

REVIEW OF CORROSION AND FUEL STABILITY UNDER IRRADIATION

G. W. Keilholtz

CAPSULE TESTS (IN-PILE)

The capsule tests are listed first because of their relative simplicity and their ability to produce statistical information. They are particularly valuable for survey work with new materials.

The principal variables which have been considered in the radiation tests of fused salts have been flux, fission power, time, and temperature. When a fixed neutron flux was available, the fission power was varied by adjusting the uranium concentration of the salt.

The properties of the irradiated salts have been examined in detail in relation to their stability. The range of conditions for the salts in Inconel containers has included thermal-neutron fluxes from about 10^{11} to over 10^{14} neutrons $\cdot$ cm^{-2} $\cdot$ sec^{-1}. The fission power has ranged from 80 to 8000 w/cc. Most tests were for 300 hr; more recent tests have been for 600 and 800 hr. Techniques of examination have included:

1. pressure tests,
2. melting-point determinations,
3. petrographic analysis,
4. chemical analysis.

These methods show that no major changes occur in the properties of the fused salts under irradiation, other than the normal burnup of uranium.

Corrosion data are about the same for irradiated and unirradiated Inconel capsules containing the fused salts. Temperatures of 2000°F and above result in penetration greater than 12 mils and are accompanied by Inconel grain growth, emphasizing the importance of close temperature control. Hot spots in any part of the fuel system must be avoided.

FORCED-FLOW LOOPS (IN-PILE)

Three types of loops have been tested in reactors (see Table 1):

1. a large horizontal loop in the lattice of the LITR, with the pump outside the reactor,
2. a smaller vertical loop operated in the lattice of the LITR,
3. a horizontal loop operating completely within a beam hole of the MTR.

Results from In-Pile Loops

The LITR horizontal loop operated for 645 hr, including 475 hr at full reactor power. The loop generated 2.8 kw, with a maximum fission power of 400 w/cc. The Reynolds number was 5000 and the ΔT was 30°F. This was a large-volume loop and therefore had a large dilution factor.

Metallographic analysis showed that less than 1 mil of corrosion occurred in the loop system. Chemical analyses showed that Fe, Cr, and Ni were each present to the extent of 200 ppm or less. Therefore, there is no evidence of accelerated corrosion in this experiment.

The LITR vertical loop operated for 130 hr, only 30 hr of this being at full reactor power. The loop generated 5 kw, with a maximum fission power of 500 w/cc. The Reynolds number was 3000 and the ΔT was 71°F. The surface-to-volume ratio was 20 in.$^{-1}$, and the dilution factor was 10. Chemical analyses showed 370 ppm Fe, 100 ppm Cr, and 50 ppm Ni. Metallographic analysis of this loop showed less than 1 mil of corrosion at the curved tip.

The MTR horizontal loop described by Trauger[1] operated for 467 hr, including 271 hr at power. The loop generated 20 kw, with a maximum power of 800 w/cc. The Reynolds number was 5000 and the ΔT was 155°F for 103 hr and 100°F for 168 hr. The dilution factor was about 5. Chemical analyses showed 240 ppm Fe, 50 ppm Cr, and 100 ppm Ni. The high iron concentration probably resulted because of a sampling difficulty. Unetched metallographic pictures of sections of the MTR horizontal loop show no corrosion penetration; the pictures of the etched specimens show that no attack was greater than 1 mil. A slight amount of intergranular void formation was noted, but this was neither dense nor deep. Measurements of wall thickness showed no variations due to corrosion. The loop has been examined carefully for any temperature effects on the inside of the bends, and no effects from overheating have been observed. Samples from the inlet, the center, and

[1] D. B. Trauger *et al.*, *ANP Quar. Prog. Rep. Sept. 10, 1955*, ORNL-1947, p 36.

TABLE 1. DATA FOR IN-PILE FORCED-FLOW LOOPS

	Horizontal Loop I	Vertical Loop II	Horizontal Loop III
Reactor	LITR	LITR	MTR
Maximum power, w/cc	400	500	800
Total power, kw	2.8	5.0	20
Dilution factor	180	10	5
Maximum temperature, °F	1500	1500	1500
ΔT, °F	30	71	155
Reynolds number	6000	3000	5000
Time in operation, hr	645	130	467
Time at power, hr	475	30	271
Corrosion, mils	<1	<1	<1
	Chemical Analysis (ppm)		
Fe			
Before	80 ± 10	90 ± 10	40 ± 10
After	180 ± 40	370 ± 20	240 ± 20
Cr			
Before	10 ± 5	80 ± 10	60 ± 10
After	150 ± 10	100 ± 20	50 ± 10
Ni			
Before	200 ± 100	145 ± 20	<40 ± 10
After	30 ± 5	50 ± 10	100 ± 20

the exit side of the loop show less than 1 mil of corrosion. The low corrosion is credited to careful temperature control of the salt-metal interface and to the fact that it was maintained below 1500°F at all times.

Future loops will be operated at higher fission powers which will result in greater values of ΔT. The dilution factors will be kept low. New fuels and new alloys are under consideration for future loop operation.

RADIATION METALLURGY

J. C. Wilson

STRESS CORROSION

W. W. Davis J. C. Wilson
J. C. Zukas

A total of eight Inconel tube-burst, stress-corrosion specimens was operated in a helium atmosphere in HB-3 of the LITR, using helium to pressurize the specimens. The circumferential stress was 2000 psi, and various test temperatures were employed. A plot of the log of time to rupture vs operating temperature (Fig. 1) revealed an unusual degree of scatter which led to investigation into the condition of the specimen tubing prior to testing. Consequently, a great deal of time was devoted to following the nondestructive testing by the Metallurgy Division of tubing to be used in subsequent tests. Of 28 tube-burst specimen tubes examined by Zyglo inspection, all but four were rejected because of pinholes and spongy regions. Metallographic inspection of 25 sections from these 24 tubes resulted in the location of only one appreciable defect, Fig. 2, on the inside of the tube. The indications of defects that show up in nondestructive testing may be partially responsible for the unusual scatter observed. In any event, about ten more specimens will be irradiated, after the stress-corrosion tests are completed, to get some idea of the distributions of rupture times in these tubes. It is believed that these data will aid in estimating the seriousness of defects in terms of creep life. The better quality tube stock for ARE radiators will probably be used in subsequent work if there are important radiation effects that need to be measured accurately. Figure 3 shows the typical structure near the fracture of one of the four in-pile, tube-burst specimens examined. Rupture occurred after 84 hr at 1500°F. Four more specimens await examination. The structure near the fracture of the only bench-test specimen available is shown in Fig. 4; time to fracture was 356 hr at 1500°F.

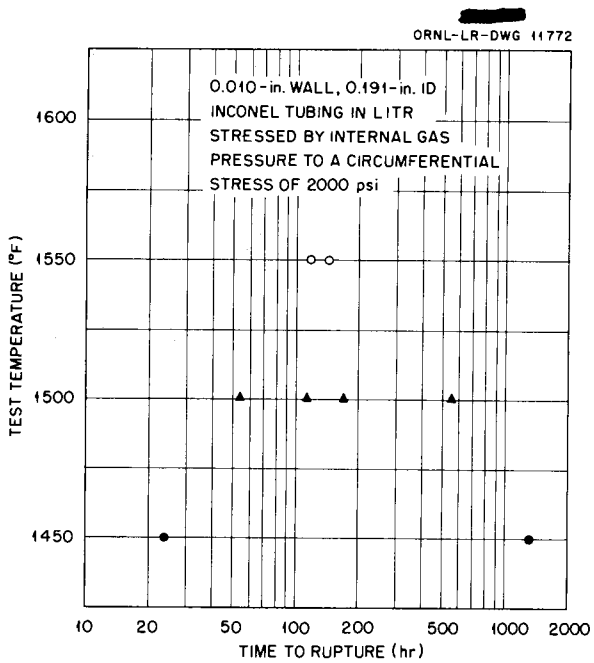

Fig. 1. Rupture Time vs Temperature for Internally Pressurized Inconel Tubes at a Stress Level of 2000 psi in Helium in the LITR.

A molten-fuel, sodium-cooled cantilever stress-corrosion rig similar to that run in the LITR[1] has been in operation on the bench for over 250 hr. Two earlier bench tests were not completed because of weld failure in one case and thermocouple failure in the other. Preparations have been made to open the irradiated sample for metallographic examination. Two more rigs of this design have been filled with fuel in the dry box and will be operated in the future.

Metallographic inspection of similar cantilever apparatus that had been operated with helium on both sides of the tube (rather than with sodium or salt) showed that some surface oxidation had taken place. There was some oxidation penetration into the grain boundaries, but this was only noticeable on the tension sides of the specimens.

Two water-cooled, finned rigs described earlier[2] have also been filled with fuel 41, and the first of these will be used to check heat-transfer calculations in the LITR.

[1] W. W. Davis *et al.*, *Solid State Semiann. Prog. Rep. Aug. 30, 1954*, ORNL-1762, p 7–8.

[2] W. W. Davis *et al.*, *Solid State Semiann. Prog. Rep. Aug. 31, 1955*, ORNL-1944, p 3.

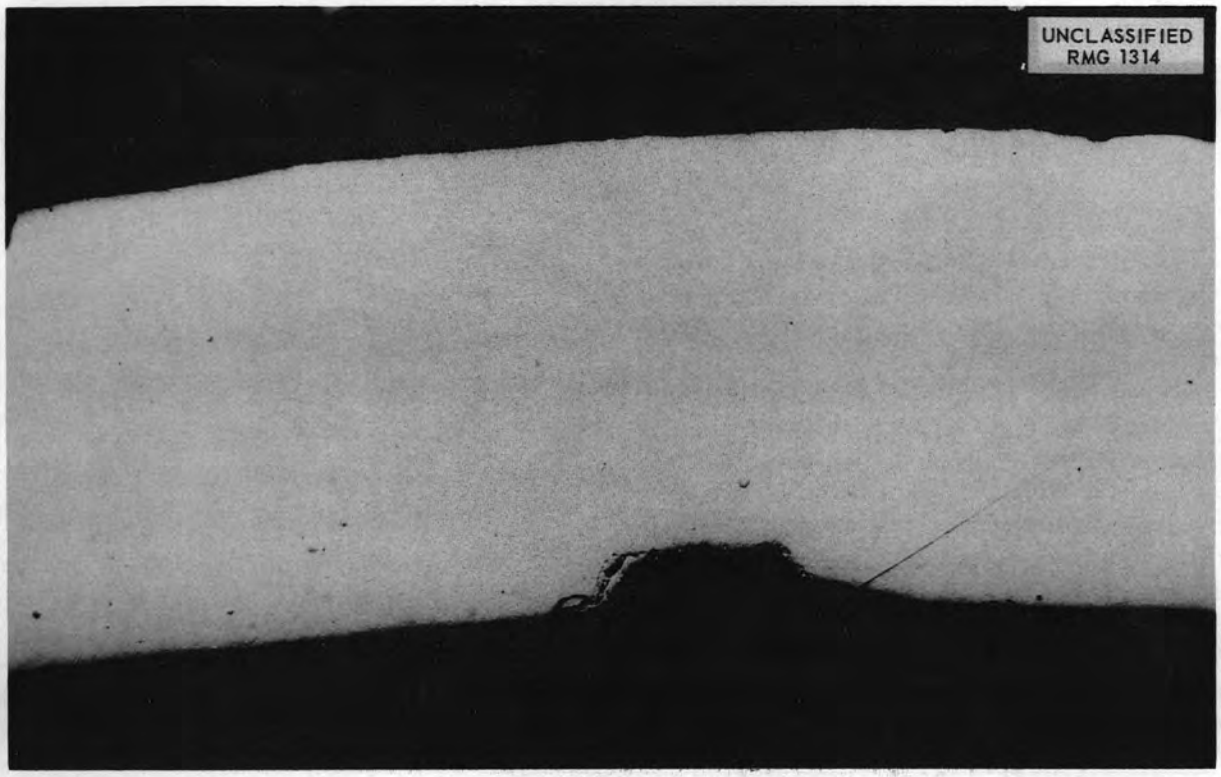

Fig. 2. Structure of Inconel Tube from Stock Used in Tube-burst Stress-Corrosion Specimens Showing a Defect Which Extended Well into the Inside Wall. 250X.

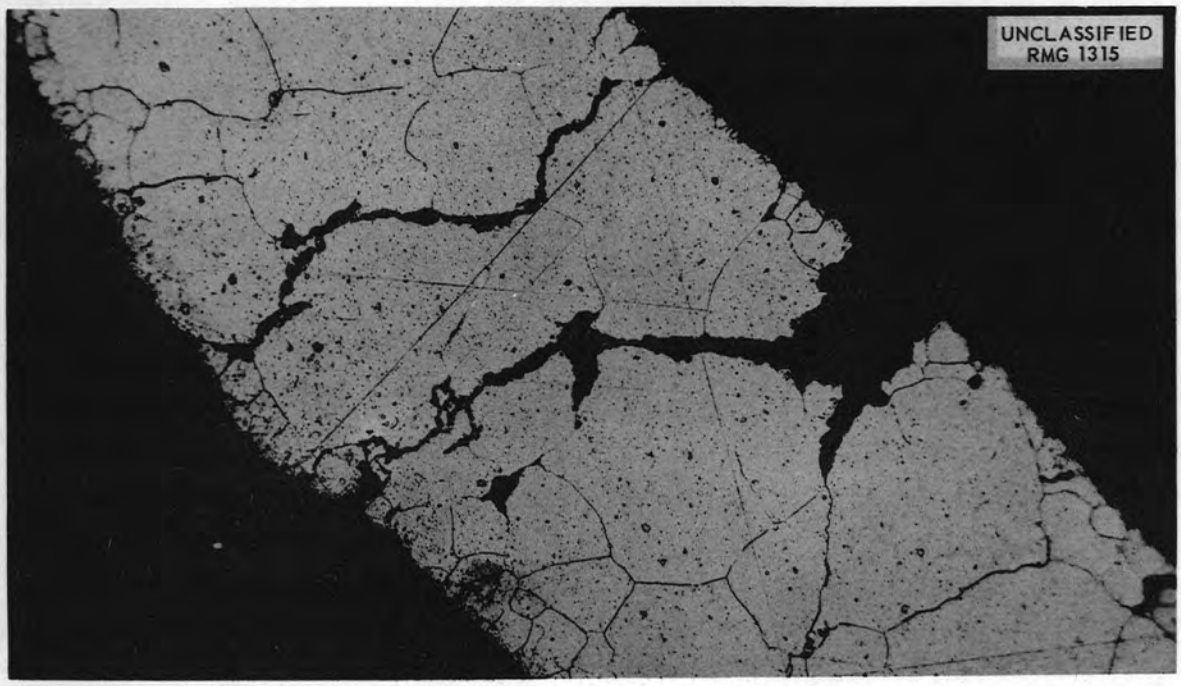

Fig. 3. Transverse Section of Inconel Tube Stressed by Internal Helium Pressure to 2000 psi Fiber Stress in LITR. Rupture occurred after 84 hr at 1500°F. Transverse section at 300X.

Fig. 4. Typical Structure of Inconel Tube Stressed by Internal Helium Pressure to 2000 psi Fiber Stress. Rupture occurred after 356 hr at 1500°F. Transverse section at 300X.

ALTERNATE STRESS-CORROSION EXPERIMENT

C. D. Baumann W. E. Brundage

An alternate method of carrying out the stress-corrosion experiment has been designed. This method retains the feature of having the molten fuel in contact with only one wall of an annular container in order to provide a small surface-to-volume ratio. Cooling the inner wall of the container will provide a frozen layer of the fuel on this surface. The specimen will be the outer wall of the container and will be stressed by pressurizing the inside of the container with helium gas. This method limits the maximum temperature of the fuel to the temperature of the specimen, 1500°F.

A preliminary design was made, based on calculations of the expected fission power, heat flow, and the limitations of fabrication. Since accurate information on the thermal-neutron flux in hole HB-3 of the LITR was lacking, a mockup of the fuel was constructed as shown in Fig. 5 and irradiated for a short time about 2 in. from the inner end of this hole. A cadmium-magnesium alloy (9% Cd, remainder Mg) was used to simulate the cross section of the fuel, and cobalt foils were used for the monitors. The foils were removed, and the activity was measured in a 100% geometry counter after irradiation.

The measurements indicate a flux of 9×10^{12} neutrons $\cdot$ cm$^{-2}\cdot$sec^{-1} at the outer surface of the fuel and 5×10^{12} neutrons $\cdot$ cm$^{-2}\cdot$sec^{-1} at the inner surface of the annulus. Calculations based on these measurements indicate an unperturbed thermal flux at this position of 2×10^{13} neutrons $\cdot$ cm$^{-2}\cdot$sec^{-1}.

The flux measurements permitted a refinement of the design to be made. Figure 6 shows the equipment now being fabricated. The platinum heater surrounding the fuel container will be used to supplement the fission heating in order to maintain the operating temperature. The outer container for the equipment will act as a safety container in case of a leak or rupture of the specimen. Power generation in the fuel will be about 750 w/cc. Postirradiation measurements will be made on the outside of the specimen tube, and the corrosion will be measured on the metallograph. The apparatus is expected to be usable in the MTR with little modification.

UNCLASSIFIED
ORNL-LR-DWG 11773

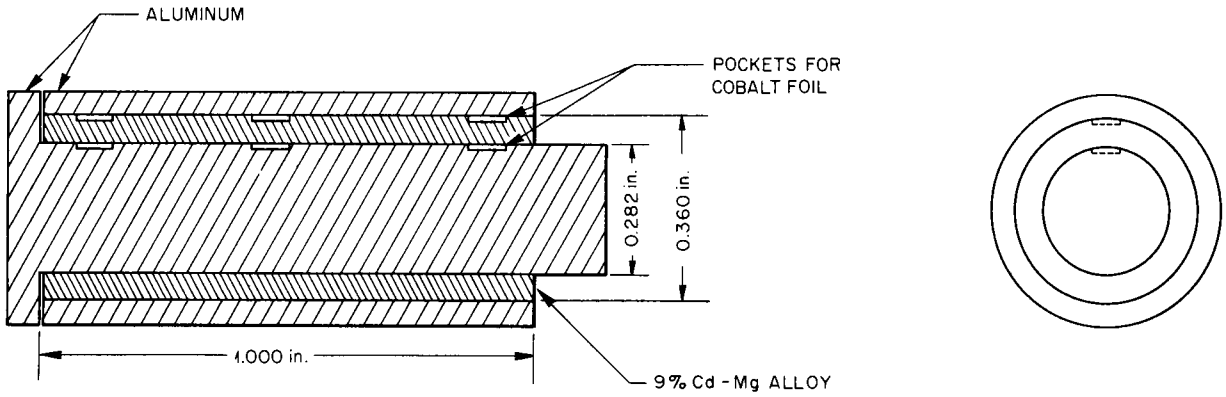

Fig. 5. Flux-Monitoring Capsule for Measuring Flux and Flux Attenuation in Mockup Stress-Corrosion Apparatus.

UNCLASSIFIED
ORNL-LR-DWG 12000

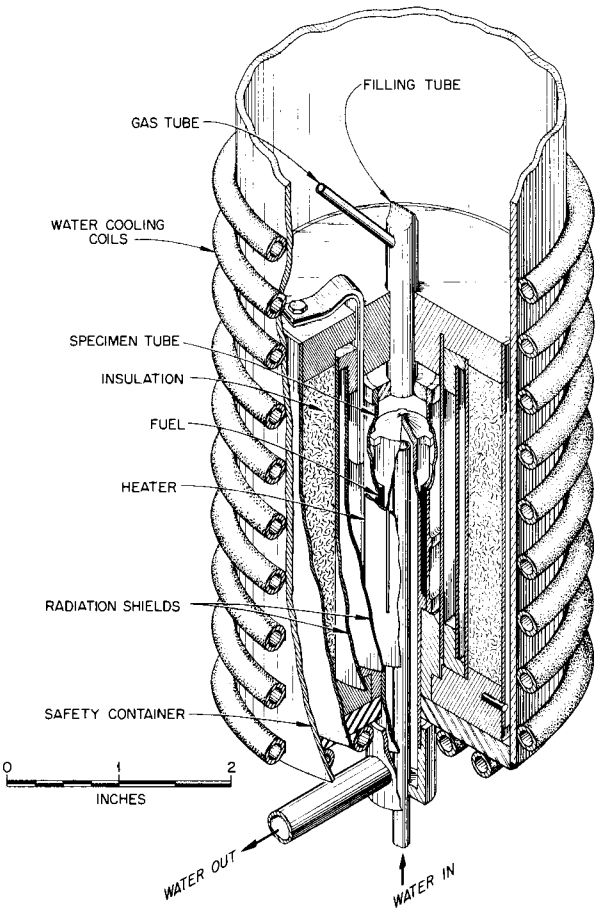

Fig. 6. Alternate Stress-Corrosion Capsule.

Considerable effort was expended in getting a new inert-atmosphere dry box into operation so that independent facilities will be available for filling and for welding of the test apparatus.

MTR TENSILE CREEP

W. W. Davis N. E. Hinkle
J. C. Wilson

The MTR tensile creep test consisted of two Inconel tubes stressed in tension to 1500 psi at 1500°F (in helium), and it was operated in hole HB-3 for 33 days at an average power level of 30 Mw. Postirradiation sectioning revealed that both specimens had fractured. Temperature measurements taken during the test showed abnormal temperature distribution after 518 hr for specimen 1, which failed outside the gage length, and after 188 hr for specimen 2, which failed within the gage length. Those portions of the specimens which were in the high-temperature region had dark surface films. The absence of metallic reflection from the fracture surfaces indicated that the specimens had not fractured during the cutting operation. Subsequent metallographic examination suggested that attack by an unknown contaminant, alone or in combination with temperature excursions, was more responsible for the short rupture life than was the neutron flux. The bench test in which conditions correspond to those of the in-pile test has been delayed by leaks in the apparatus.

Metallographic examination of irradiated specimen 2 revealed an intergranular fracture, and necking

at the point of failure. Photomicrographs of longitudinal sections showed that there was considerable internal grain-boundary separation. The incidence of grain-boundary separation appeared greatest adjacent to the fracture and decreased with increasing distance from the fracture. Surface grain-boundary separation was observed at the inside surface to a maximum depth of 0.004 in. in a few places.

Photomicrographs of sections adjacent to the fracture show the presence of an unidentified film on the specimen surface. This film is thicker on the inside surface of the specimen tube. Fracture surfaces and surface grain-boundary separations exhibit the film, but internal separations do not.

Sulfur attack, because of its well-known effects on nickel alloys, was thought to be a possible cause of the surface film and the intergranular attack observed in the photomicrographs. Finding the source of the contaminant is important so that it can be eliminated from future apparatus. No indications of sulfur were found in the wire insulation or in the specimen furnace insulation. An attempt to reproduce the surface film on the irradiated specimens was made by heating a similar Inconel tube in contact with sulfur for a short time near 1500°F. Observation of the region contacted by the sulfur revealed a large amount of grain-boundary penetration, compared with the limited amount of surface film seen in the surface grain-boundary separation in the irradiated specimen. Sulfur printing techniques were applied to the control sample without success.

Inconel tubing used for specimen stock was subjected to ultrasonic and to eddy-current tests by the Metallurgy Division. These tests showed indications of defects. Samples were cut from the regions classed as most defective, but metallographic examination did not reveal any observable defects.

Analysis will continue with the measurement of the creep strain of specimen 1, sectioning of specimen 1 for metallographic examination, and x-ray analysis of the surface film.

PNEUMATIC STRESSING DEVICE

A. S. Olson J. C. Wilson

A pneumatic stressing device has been designed to provide a powerful, compact means of stressing creep specimens with loads as great as 10,000 lb. The device can be used for creep, stress-corrosion, and stress-relaxation tests both in the laboratory and in in-pile experiments. The prints are in the shop. Work continues on a suitable recording creep extensometer.

DUCTILITY OF NICKEL ALLOYS

T. C. Price J. C. Wilson

The ductility minimum that frequently occurs in tension test results from nickel alloys in the neighborhood of 1000°F is being studied. First, the effect of strain rate is being measured. To date, fairly complete data have been obtained for monel; and work on Nichrome and Inconel is under way.

The gage-length portion of the tension specimens is 0.1500 ± 0.0005 in. in diameter and 0.60 ± 0.05 in. in length. Two strain rates were used: 2 and 0.002 in./min. The test temperature ranged from 800 to 1400°F. The ultimate and yield strengths at both strain rates seemed to vary linearly with temperature. There was, however, a large nonlinear decrease in elongation and in percentage reduction of area in the region 900 to 1000°F at the faster strain rate (see Figs. 7 and 8). This anomaly was not observable at the slower strain rate.

At the lower strain rate the ductility values are lower than for the faster rates. At about 1000°F the ductility values nearly coincide for both strain rates, so the processes responsible for the behavior are independent of strain rate at this temperature. At higher and lower temperatures the curves tend to diverge, with the higher strain-rate curves showing greater ductility.

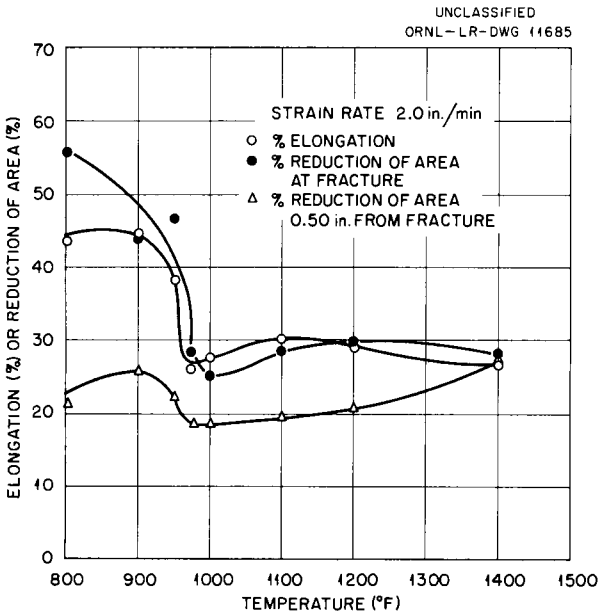

Fig. 7. Effect of Temperature on Tensile Ductility in Monel at Strain Rate of 2.0 in./min.

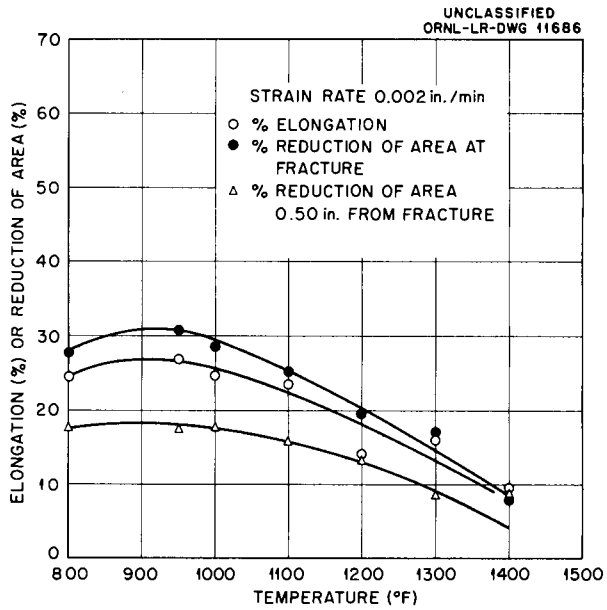

Fig. 8. Effect of Temperature on Tensile Ductility in Monel at Strain Rate of 0.002 in./min.

ENGINEERING PROPERTIES

O. Sisman

RADIATION DAMAGE TO CERAMIC FUEL MATERIALS

J. G. Morgan R. M. Carroll
M. T. Morgan

The study[1] of engineering properties of irradiated, solid, ceramic fuel materials has two major objectives: (1) the determination of the effects of reactor radiation on the physical properties of ceramic fuels and (2) the establishment of design criteria for maximum radiation stability of these fuels. The four principal reasons for emphasizing ceramic fuels are: they may be used at high operating temperature (above 2000°F); the two basic fuel materials are ceramics (UO_2 and ThO_2); they are available; they are economical. The fuel-element materials now being investigated are SiC-Si-UO_2 and ThO_2-UO_2. The SiC-Si-UO_2 fuel element has especially attractive physical properties at elevated temperatures (up to 2200°F). Specifications in reactor design studies recommend that this element be used as a thin plate.[2] The silicon carbide and uranium oxide exist in a matrix of silicon. The outer surface layer contains no uranium oxide and acts to retain fission products.

The thorium oxide–uranium oxide fuel element has the advantage of a longer effective life due to the production of U^{233}; ThO_2 forms a solid solution with UO_2 throughout the entire range of compositions.[3] The body can be fabricated in various geometries and forms a hard, strong, impervious structure.

Test equipment has been constructed to measure property changes as a result of irradiation. The properties after irradiation will be measured in the hot cell and include density, dimensional stability, specific heat, x-ray diffraction, breaking strength, and Young's modulus. Microscopic examination will be used to reveal cracks, voids, and grain-size changes. One of the characteristics desirable in the fuel-element materials is fission-product retention so as to avoid contamination of the reactor coolant. Procedures have been developed for piercing the capsule containing the sample and for analyzing the released gas for fission products.

Currently, SiC-Si-UO_2 fuel plates are being exposed in facility C-48 of the LITR. The plates, containing 4 wt % uranium (enriched), are maintained at temperature by fission heat generation in a helium atmosphere. Figure 9 shows such a plate, together with x-ray photographs which outline the UO_2 matrix. Figure 10 shows the sample in its irradiation capsule. The gas-analysis tube is weld-sealed with a foil which will be later pierced for the fission-gas determination. The sample, in a thermal flux of 2.5×10^{13} *nv*, generates about 120 w/in.^{2} and is maintained at a temperature of 1750°F. A preliminary run at 2.7 ×

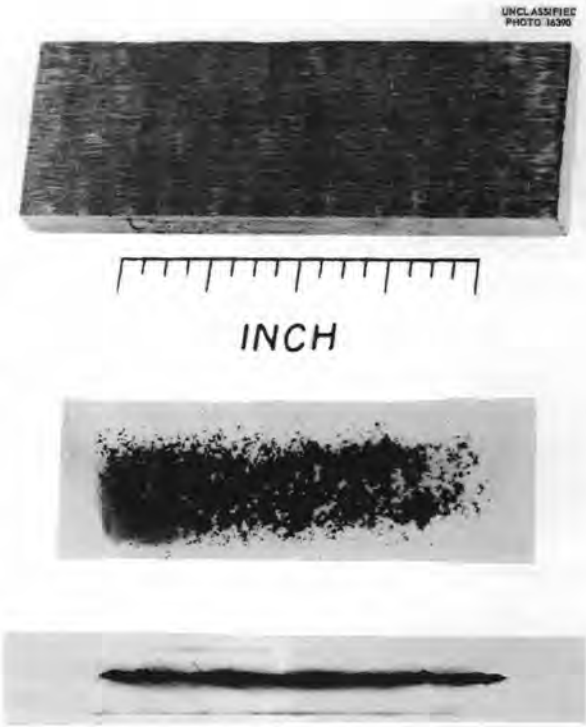

Fig. 9. SiC-Si-UO_2 Fuel Element. (Secret with caption)

[1] J. G. Morgan and O. Sisman, *Radiation Damage Studies of Ceramic Fuel Elements*, ORNL CF-55-7-12 (July 6, 1955).

[2] J. G. Gallagher *et al.*, *Gas Cooled Ceramic Package Reactor*, ORNL CF-53-10-30 (Sept. 1953).

[3] J. Stravrolakis and H. N. Barr, *Appraisal of Uranium Oxides*, TID-5150 (Aug. 3, 1953).

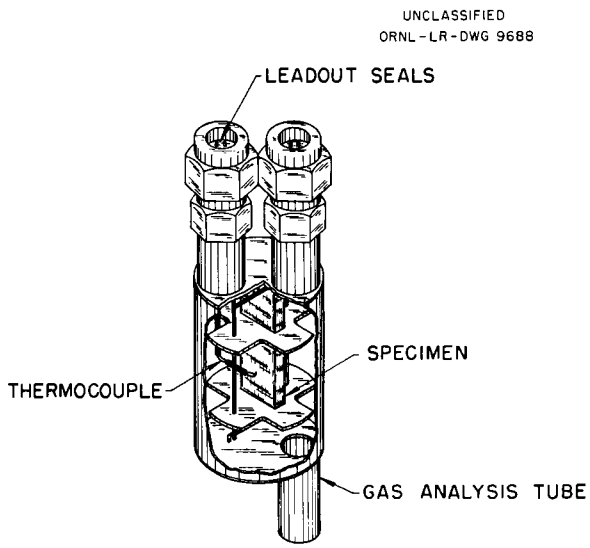

Fig. 10. Ceramic-Sample Capsule.

10^{17} *nvt* and at 1750°F revealed no physical change in the sample.

Furnace and Calorimeter for Remote Determination of Specific Heat

Heat capacity may be determined by many methods. The apparatus for this experiment was chosen because it was most easily adaptable to remote operation. Because high-temperature determinations of heat capacity were desired, it was impractical to design a closed system in which a measured amount of energy could be added in order to obtain a measured temperature rise. The most rugged apparatus of the external calorimeter type appeared to be one using the copper-block method. The apparatus is, most simply, an insulated copper block of a mass large in comparison with the mass of the sample. The sample is heated to a desired temperature and is then placed in a cavity in the copper block. When the sample attains thermal equilibrium with the block, the temperature of the block has been increased, ideally, by an amount dependent upon the mass of the block, the mass of the sample, the initial temperature of the sample, and the heat capacity of the sample. It is apparent that the accuracy of the copper-block method will depend upon the adiabatic condition of the copper block, the sensitivity and accuracy of the temperature measurements, and the accuracy of determination of the temperature at the moment the sample is placed in the calorimeter.

The adiabatic condition of the calorimeter requires an environment that will change temperature at the same rate as the copper block and which will retain a constant temperature when the copper block is at equilibrium. Electric heating is the simplest method for doing this but has the disadvantage that any overshoot in environment temperature can only be corrected by the dissipation of heat, some of which may be transmitted to the copper block. An additional disadvantage of electric heating is that an auxiliary cooling system must be used to bring the calorimeter insulation to a lower temperature after several successive tests. For these reasons it was decided to control the temperature of the copper-block environment with circulating water. The temperature of the circulating water is regulated by controlled mixing of hot and cold water. The source of the hot and cold water may be the usual plant supply.

The construction of the copper-block calorimeter is shown in Fig. 11. A hole $\frac{3}{4}$ in. in diameter and 3 in. deep was drilled in a cylindrical block of copper of the desired mass. Eight thermocouple wells of varying depth were spaced about the outside of the block. A stainless steel tube $\frac{3}{4}$ in. ID was brazed to the copper block so that it could be suspended inside a copper cylindrical tank. The surfaces of the copper block and the inside of the copper tank were bright-nickel-plated in order to reduce heat transfer by radiation. Small thermocouple wells, spaced about the inside of the tank, accommodate a differential thermopile, with the eight junctions in the copper block. The thermocouples in the block serve to determine the average temperature of the block. Lead wires from the thermocouples were passed out of the tank through Kovar seals, and the space between the tank and block was evacuated to reduce heat transfer by conduction. The controlled-temperature water passes through copper tubing which is spiralled about the outside surface of the copper tank. To aid in heat transfer between the copper tubing and the copper tank, the entire assembly was placed in a snug-fitting steel tank, and the annulus between the steel tank and the copper tank was filled with ethylene glycol. The steel tank was then placed in an insulated container.

To minimize the heat loss in transferring the sample from the furnace to the calorimeter and to make it more nearly constant, the drop method of sample transfer was used. In this method, a

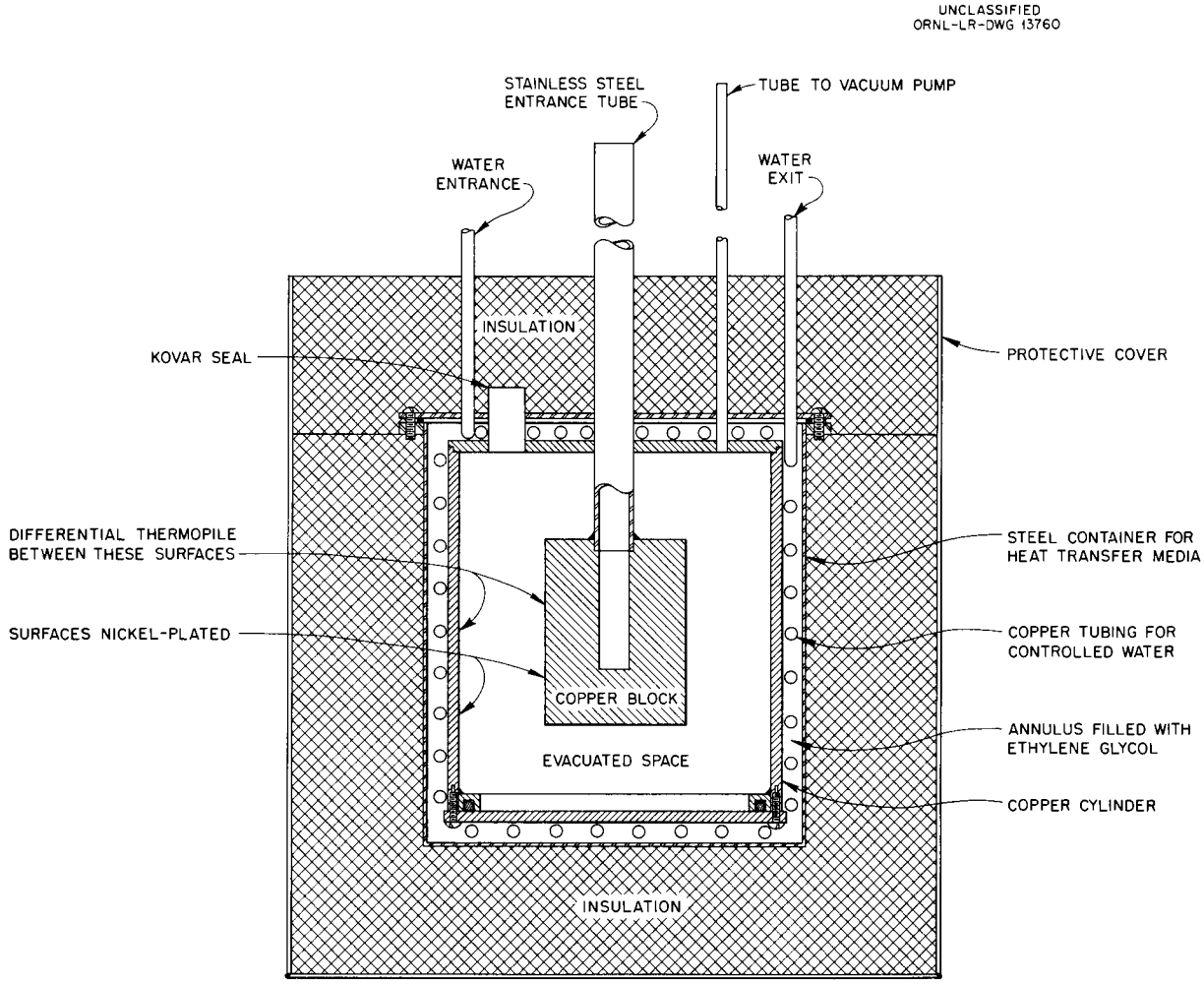

Fig. 11. Copper-Block Calorimeter.

tube furnace, with its long axis vertical, is suspended above the calorimeter, and the sample is dropped in free fall from the center of the furnace to the calorimeter. The furnace (Fig. 12) was constructed with platinum wire wound about an alundum tube, which was machine-grooved to ensure even spacing of the windings. To avoid thermal gradients along the length of the furnace tube, the furnace was constructed with three separate windings in tandem. Nine thermocouples were installed along the length of the furnace, three for each winding. These thermocouples were placed through holes drilled between the heater coils so that the junctions were flush with the inside surface of the furnace. The center heater winding was constructed sufficiently long so as to easily contain the sample. The two end heaters are maintained at the same temperature as that in the center heater in order to eliminate end effects.

The sample is suspended in the furnace by means of a ceramic support rod which protrudes into the furnace tube through a ceramic tube (see Fig. 13). The furnace is mounted on a pivot so that it can be swung 180 deg away from the calorimeter when the sample is loaded and when the calorimeter is unloaded. Suitable stops position the furnace. A telescoping steel tube is used to raise a sample into the furnace. With the sample in position, the support rod can be pushed under the sample and the tube lowered. The bottom of the furnace is

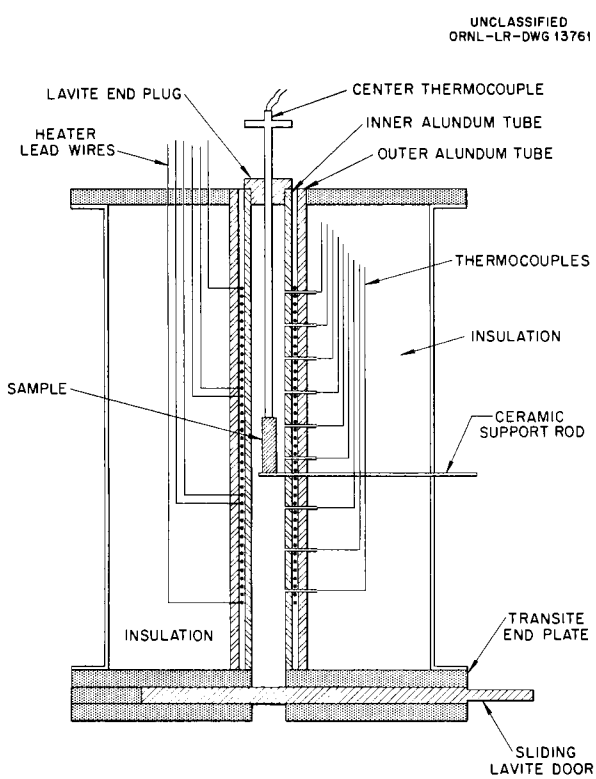

Fig. 12. Specific-Heat Furnace.

fitted with a sliding Lavite door. The thermocouples spaced along the furnace tube are used to ensure uniform temperatures along the length of the tube. The actual furnace temperature is measured with a central thermocouple mounted on a probe which extends axially through the furnace. This probe, containing two thermocouples, presses directly against the sample by force of gravity.

Instrumentation for the furnace and calorimeter is shown in Fig. 14. The output of the differential thermopile between the copper block and the surrounding tank is fed to a recorder-controller which controls air pressure transmitted to pressure-controlled water valves for the hot and cold water. The water, after passing through the regulating valve, enters a mixing manifold and from there passes into the copper coils surrounding the tank. The water capacity of the system is small to allow for rapid changes. A semimanual control is used at the time of dropping of the sample so that a surge of hot water may be passed into the system just before the hot sample is dropped. The output of the thermopile from the copper block is fed into a multirange single-pen recorder. When the recorder indicates that an equilibrium has been attained, the output of the thermopile is switched to a potentiometer for more accurate readings. The potentiometer may also be used to measure the temperature of the furnace central probe. The furnace temperature is controlled by an automatic electrical controller which receives the output of one of the thermal probes. The controlled voltage is fed into three Variacs, each of which is connected to one of the furnace coils.

When the specimen is dropped into the calorimeter, there is an initial surge of heat into the copper block. This is compensated for by adding hot water manually to the system just before the drop, as discussed above. At no time during the tests did the temperature of the block vary from its surroundings by as much as 1°C, or more than 0.5°C for as long as 1 min. As soon as conditions near equilibrium are established (generally within 1 min), the automatic control is used. This generally controls the temperature of the cylinder surrounding the copper block to within 0.1°C, with an oscillation (period of about 1 min) about the zero differential temperature. Measurements of the calorimeter drift indicated about 0.03°C drift per hour, which is the limit of accuracy of the potentiometer. The calorimetry system was calibrated by dropping synthetic sapphire samples in a platinum container into the calorimeter. The reproducibility of the calorimeter and furnace system is about 1.5%.

RADIATION DAMAGE TO BORON CARBIDE

J. G. Morgan R. M. Carroll
M. T. Morgan

A program is under way to study radiation effects on B_4C and related ANP thermal-neutron shields. The first irradiations were made on uncoated, hot-pressed B_4C (Norbide) and cold-pressed B_4C bonded with SiC (Carborundum Co.). The samples, sealed under helium in quartz ampoules, were exposed in facility C-48 of the LITR to 6×10^{19} *nvt* (as measured by cobalt foil activation at the surface of the specimen). The samples were placed in a perforated aluminum container and cooled by the reactor water. Figure 15 shows the samples and their container; the upper samples were the hot-pressed material. Final burnup figures will be obtained by analysis of the B^{10}/B^{11} ratio. After irradiation, the ampoules were broken, and

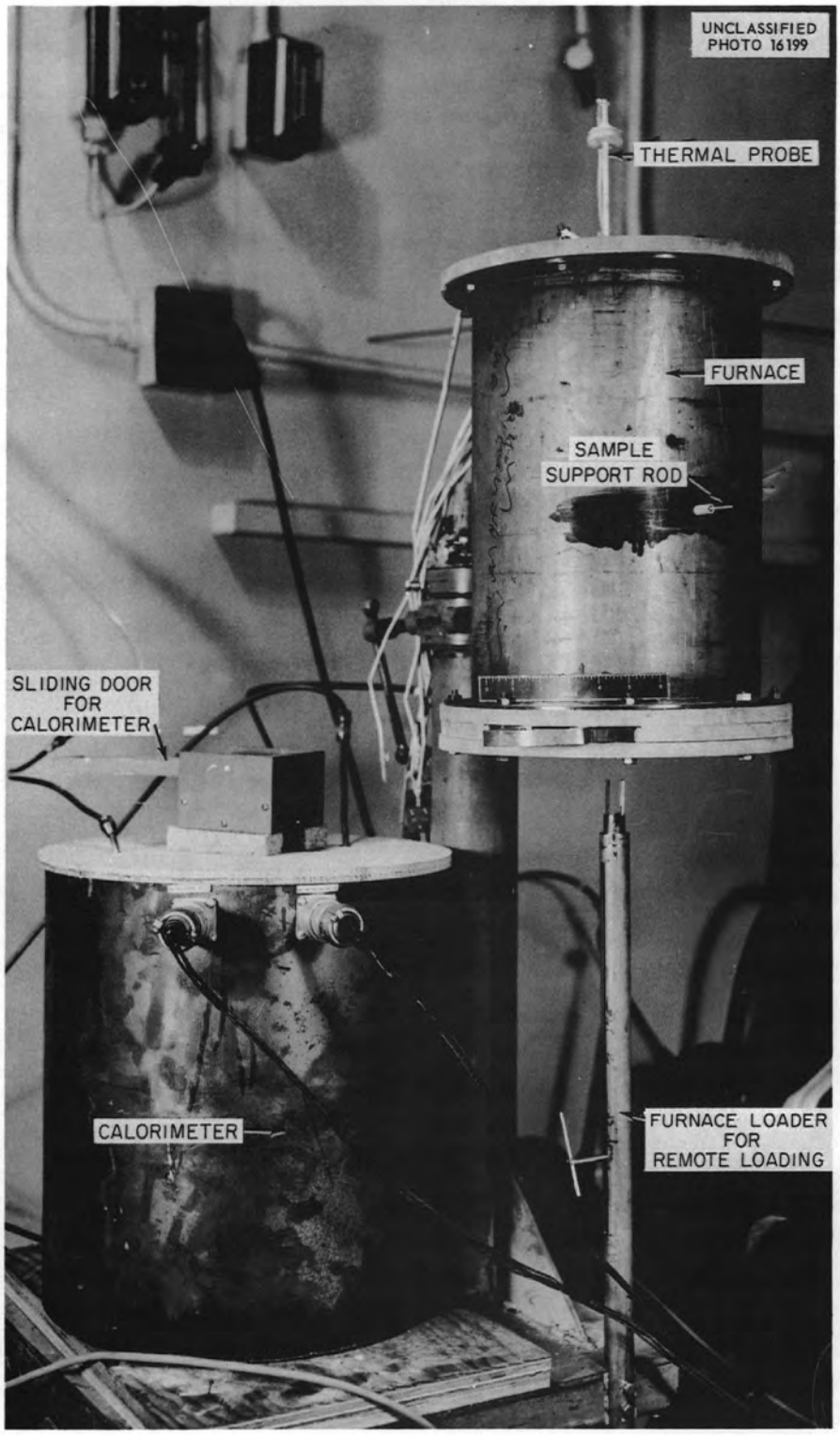

Fig. 13. Remotely Operated Specific-Heat Apparatus.

the gas released from the sample was measured. The ampoule opener is shown in Fig. 16. The ram is struck, breaking the ampoule and releasing the gas into a measured volume. By use of the manometer with the adjustable head, Fig. 17, the gas formed as the result of irradiation is determined by measuring the change in volume with change in pressure.

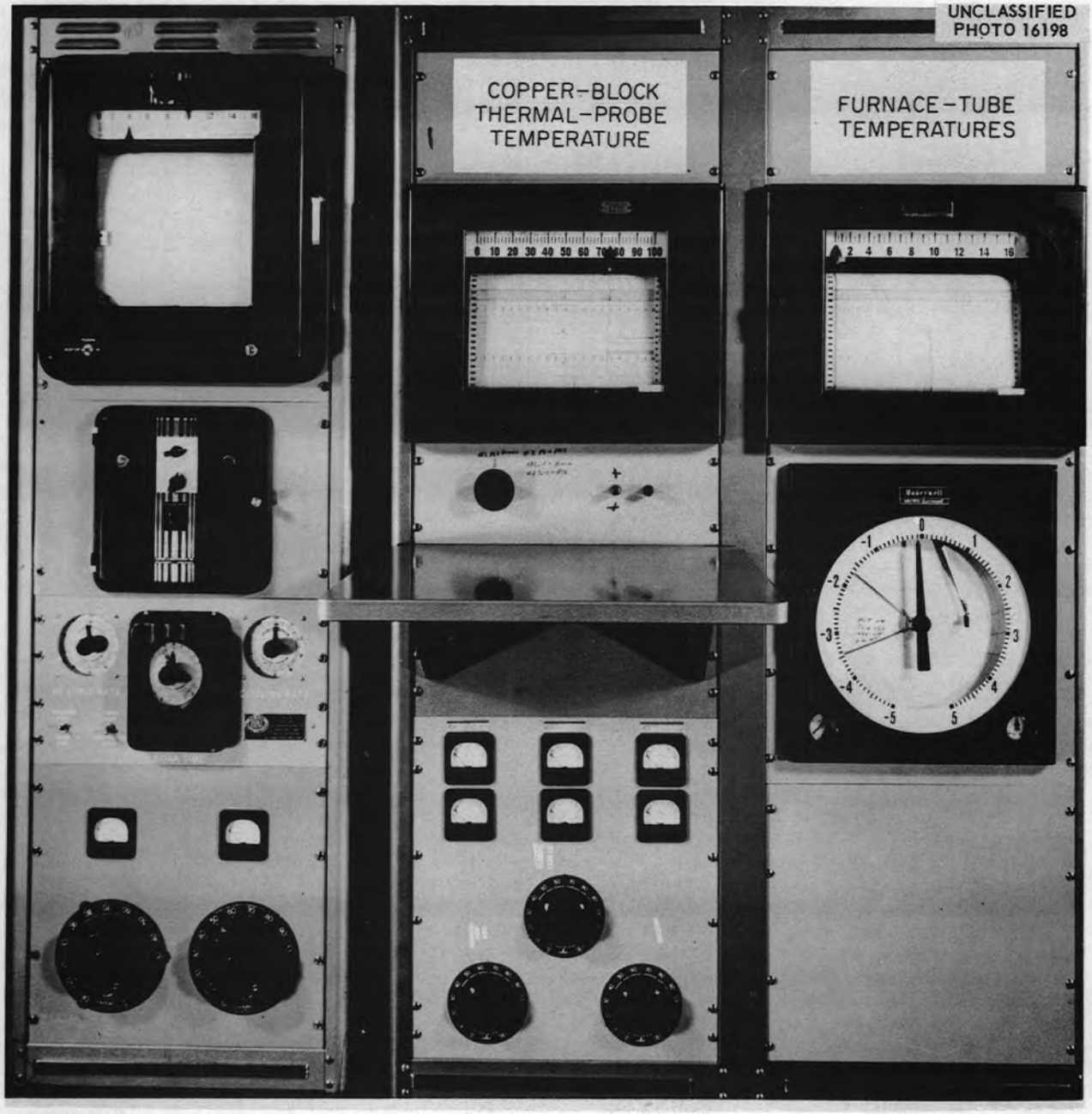

FURNACE TEMPERATURE CONTROLLER-RECORDER

VARIACS FOR TEMPERATURE EQUALIZATION

CONTROLLER-RECORDER FOR CALORIMETER

Fig. 14. Specific-Heat Instrumentation.

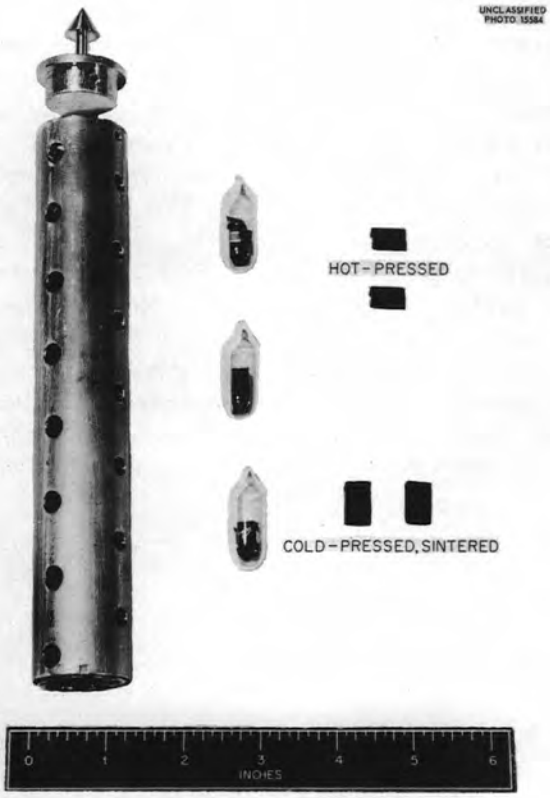

Fig. 15. Boron Carbide Specimens and Irradiation Assembly.

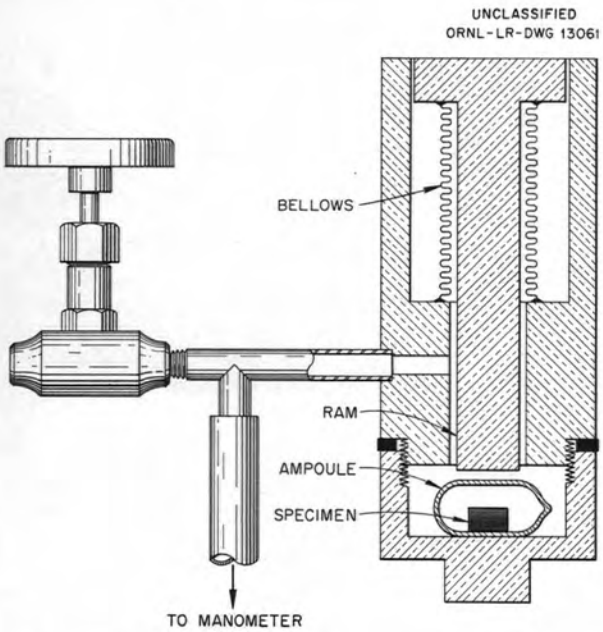

Fig. 16. Gas-Release Apparatus – Ampoule Opener.

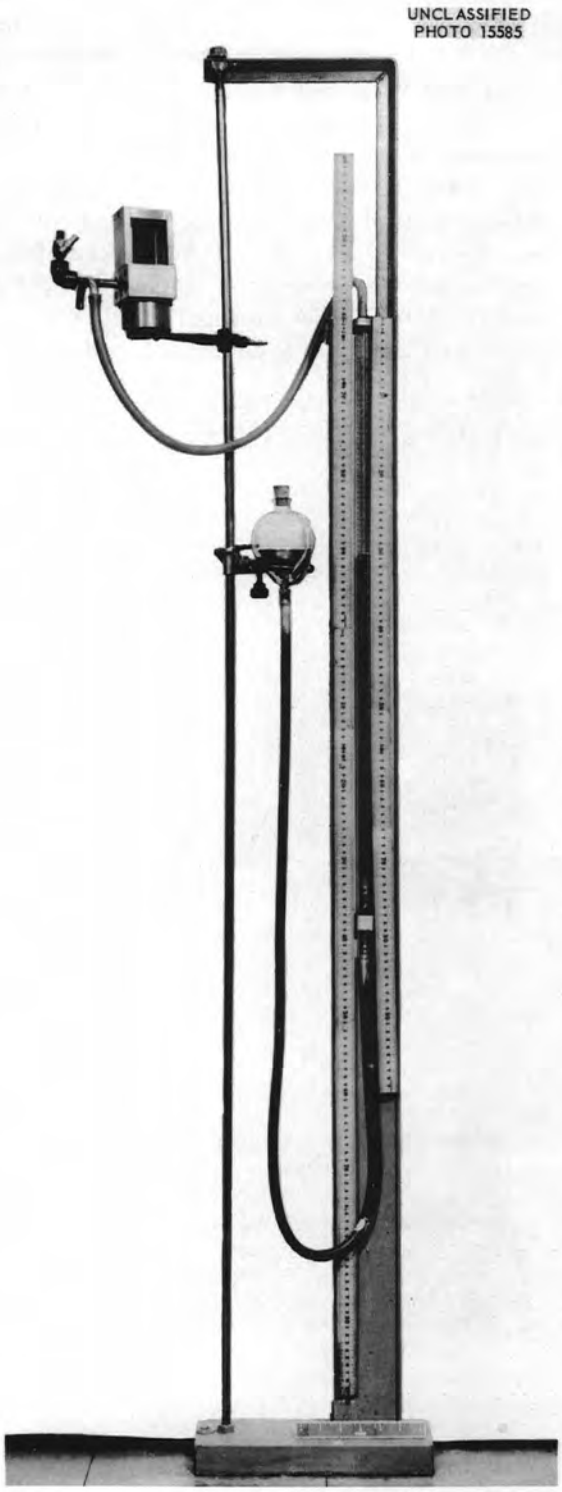

Fig. 17. Gas-Release Apparatus.

Previous work[4] indicates that most of the helium produced from the n,α reaction with B^{10} in hot-pressed B_4C is released at elevated temperatures (above 1500°F). The results bore this out, as no helium evolution as the result of irradiation was noted for the hot-pressed material within the limits of the apparatus (±0.2 cc). The hot-pressed samples retained their physical dimensions and bulk structure (Fig. 18). It was expected that crumbling of the hot-pressed material[4] might be observed at the higher burnups. With the cold-pressed and sintered B_4C (bonded with SiC), a different effect was noted. While the material itself appeared to retain its bulk stability, there was a release of gas (under irradiation) which far exceeded the total helium generation. In addition, the walls of the quartz ampoule were coated with a heavy black deposit (see Fig. 19), resulting in a 4% sample-weight decrease. This condition was not obtained when unirradiated specimens were heated for 72 hr at 1800°F. Probably, the method of fabrication resulted in some foreign material (organic binder or pitch) remaining in the sample.

In order to determine if the hot-pressed samples retain helium at elevated temperatures, gas release will be measured at temperatures up to 2150°F on the irradiated samples. In addition, the following

[4] W. D. Valovage, *Effect of Irradiation on Hot-Pressed Boron Carbide*, KAPL-1403 (Nov. 15, 1955).

UNCLASSIFIED
PHOTO 16273

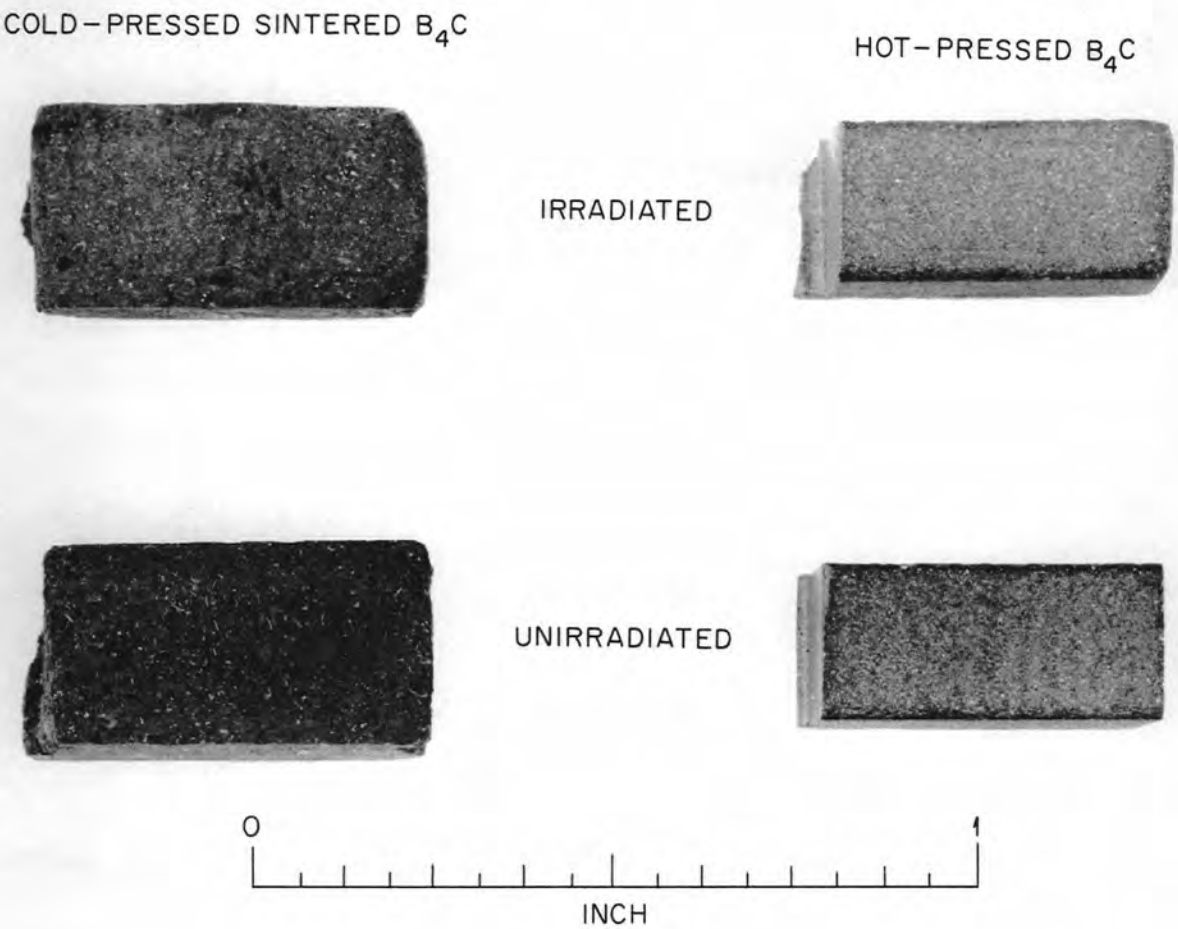

Fig. 18. Comparison of Irradiated and Nonirradiated B_4C. 3X.

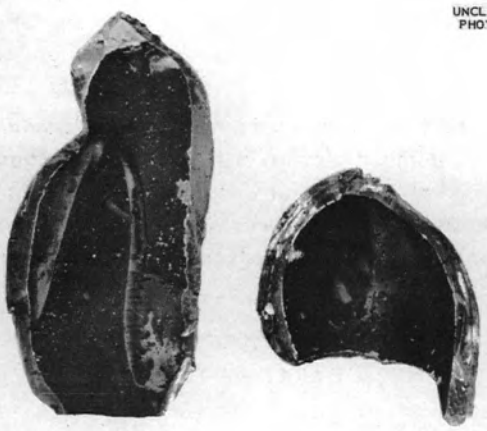

Fig. 19. Coating Inside Cold-Pressed, Sintered B_4C Ampoule After Irradiation.

boron-containing materials are of interest and will be investigated:

1. 2% B-Fe alloy,
2. 29.75% B_4C bonded with copper and flame-coated with copper and stainless steel,
3. 89% B_4C bonded with SiC and flame-coated with copper and type 410 stainless steel,
4. B_4C bonded with carbon and flame-coated with Al_2O_3.

Coating adherence, dimensional stability, and helium evolution will be studied under irradiation at elevated temperatures. Future irradiations will be made at the MTR at temperatures up to 2000°F and with radiation exposures of 10^{20} *nvt* and greater.

REACTOR EXPERIMENTS

W. E. Browning

EFFECT OF RADIATION ON STATIC CORROSION BY FUSED SALT

W. E. Browning H. L. Hemphill

Irradiation of Inconel capsules containing various fused-salt fuels was continued for the purpose of determining the corrosion behavior during fission of the fuel. Since early tests[1] showed that no significant effect on corrosion had occurred in irradiated capsules after two weeks in the MTR, emphasis was placed on longer tests. Seven capsules were run in the past year for six or nine weeks at 1500°F with NaF, ZrF_4, and 2 mole % UF_4, 2 mole % UF_3, or 4 mole % UF_4. These capsules are in the process of being sampled for metallography and for chemical analysis. Capsules containing 4 mole % UF_4 fuel are being prepared for irradiation in the MTR at 1800°F. One of these capsules is being tested at 1800°F in the laboratory in order to ensure that good corrosion results in the absence of radiation can be expected.

A multicapsule facility has been established in the MTR in a hitherto unused high-flux position.

The temperature-control system previously described[2] has performed satisfactorily for more than a year. Three identical units are now in service. Various unforeseen disturbances have been handled without excessively affecting the capsule temperature, including one in which droplets of water were sprayed intermittently on a capsule operating at 1500°F.

The thermocouples previously described[3] also have served satisfactorily. Of approximately 25 thermocouples of this type used in the MTR, only one failed. One of three thermocouples failed when sprayed, while hot, with liquid water after six weeks of irradiation, while the other two survived.

Mockup tests simulating MTR capsule conditions were run on samples of Hastelloy B in order to determine whether oxide scaling on the outside could be prevented so as to eliminate contamination. Chromium plating of the outside of capsules produced a coating that was adherent in air at high temperature and which was similar to that found on Inconel. This plating appeared to be promising for use with present MTR capsule design.

HOLDUP OF FISSION GASES BY CHARCOAL TRAPS

W. E. Browning C. C. Bolta[4]

Charcoal traps are used to retain or delay fission gases from in-pile loops circulating fused-salts and will be used on the Aircraft Reactor Test. For proper trap design it is important to know the ways in which various factors affect trap performance. A study has been undertaken to determine these relationships.

The purpose of the charcoal traps is to limit to a safe level the rate at which activity is vented to the atmosphere. The traps reduce the amount of activity by holding it up while it decays, and they reduce the rate of activity release by spreading it out over a long period of time. To determine the amount of activity leaving the traps as a function of time, the time the radioactive gases are delayed (holdup time) in the traps must be known, as well as the length of time over which they are released. Both factors for a given gas are a function of trap geometry, type and amount of charcoal, trap temperature, and type and flow rate of inert purging gas.

An experiment was set up, Fig. 20, using radiokrypton as the least adsorbed of the fission gases. Two purging gases, nitrogen and helium, were used to sweep the radiokrypton through the trap. The trap was made from 2-in. sched 40 stainless steel pipe and was 13 in. long; it contained $\frac{3}{4}$ lb of 8- to 14-mesh Columbia ACA charcoal. Trap temperatures were kept constant by using freezing solutions of $CaCl_2$ brine for the −50°C level, and a freezing solution of Freon 11 and 22 for the −110°C temperature. Liquid nitrogen was used to keep the material at its freezing point.

For each run, the trap was filled with purge gas, the manifold was evacuated, and radiokrypton was allowed to flow into the krypton chamber. The

[1] W. E. Browning, *Solid State Semiann. Prog. Rep. Aug. 30, 1954*, ORNL-1762, p 39; W. E. Browning and H. L. Hemphill, *Solid State Semiann. Prog. Rep. Feb. 28, 1955*, ORNL-1851, p 18.

[2] W. E. Browning and H. L. Hemphill, *Solid State Semiann. Prog. Rep. Feb. 28, 1955*, ORNL-1851, p 19.

[3] *Ibid.*, p 20.

[4] Aircraft Reactor Engineering Division.

UNCLASSIFIED
ORNL-LR-DWG 13762

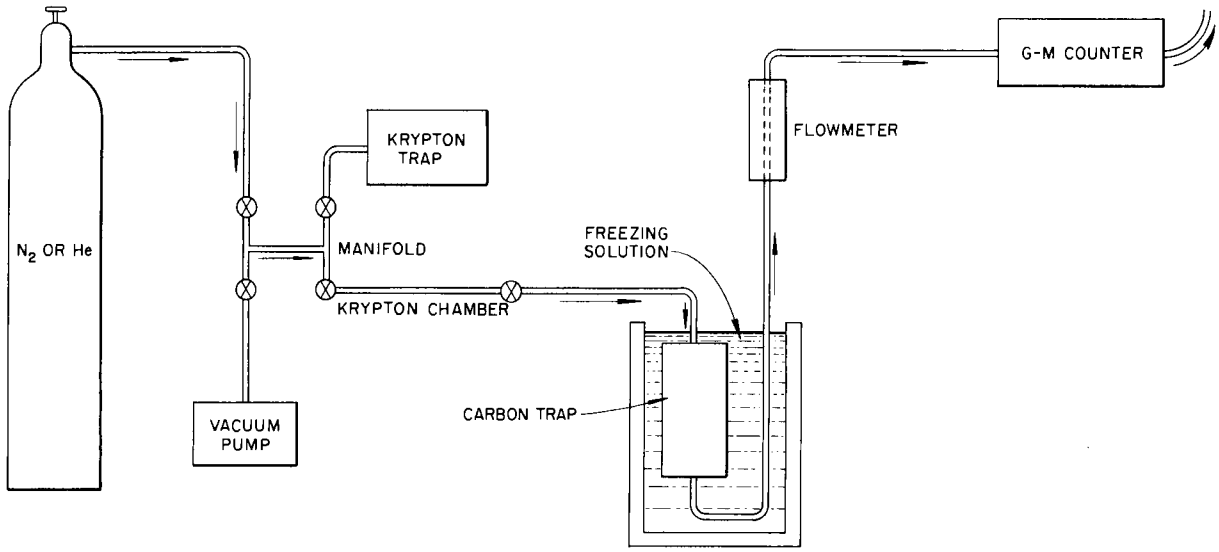

Fig. 20. Apparatus for Carbon-Trap Experiment.

chamber was sealed and the rest of the manifold evacuated. Purge gas was then allowed to push the radiokrypton into the traps at a constant flow rate of 5 ft^3/hr. The concentration of radiokrypton in the effluent gas and, therefore, its partial pressure can be determined by measuring the activity of the gas. The relative activity of the effluent gas was measured as it passed through a small cell, one wall of which was the end window of a Geiger tube. The gas activity was registered on a log counting-rate recorder.

Figures 21–24 show the results obtained for nitrogen purge gas by using one trap, and two identical traps in series, at +16, +5, −51, and −110°C, respectively. In each case the activity injected was determined by integration of the activity vs time curves; all results were normalized to the same area under the curve. It can be seen that for a given trap geometry the holdup times (i.e., time for activity to break through), time for activity to peak, and time for last appearance of activity, increase with decreasing temperature. This can be predicted, since the energy of a gas molecule is less at low temperature and the molecule cannot as readily desorb from the charcoal surface into the moving gas stream. The maximum concentration of radiokrypton in the effluent gas is lower for lower temperatures.

The curves show that the time to peak for two identical traps in series with nitrogen purge gas is approximately twice as long as for one trap and that the break-through time is from twice as long to three times as long as for one trap. The time to the end of the effluent activity is also increased, and the maximum radiokrypton concentration is reduced.

Similar curves were obtained for helium purge gas (see Fig. 25). The shapes of these curves are somewhat uncertain, since their accuracy was limited by the sensitivity of the flowmeter in its lower range when used with helium. Several runs were made at each temperature, and the holdup times measured were significant, even though the exact shape of the curve may be in doubt. These curves show that radiokrypton is held up for much longer periods of time in the presence of flowing helium than in the presence of flowing nitrogen. Since nitrogen is itself adsorbed in large amounts on charcoal, the charcoal surface is not as free to adsorb krypton. Helium will pass over charcoal with very little adsorption. Hence, krypton is retained on the charcoal for longer periods of time in the presence of flowing helium.

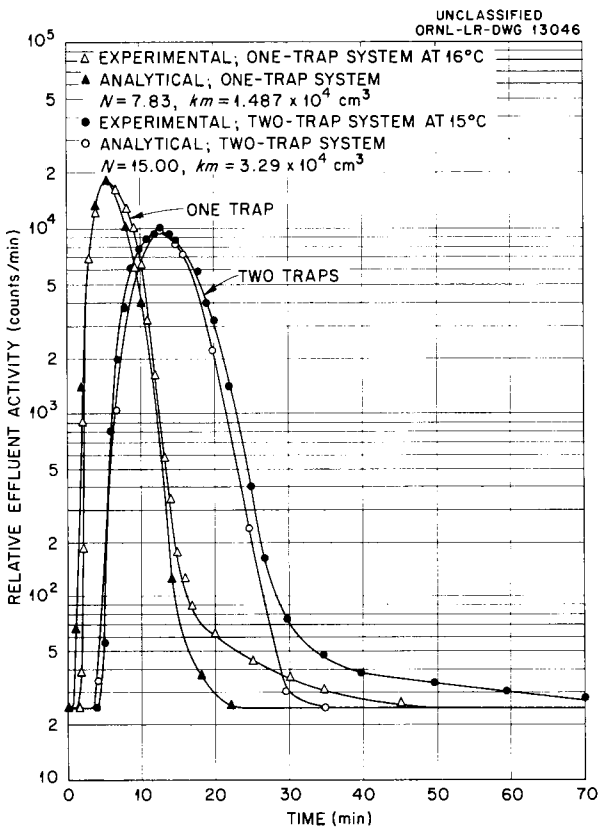

Fig. 21. Holdup of Radiokrypton in Charcoal Traps – N_2 Purge.

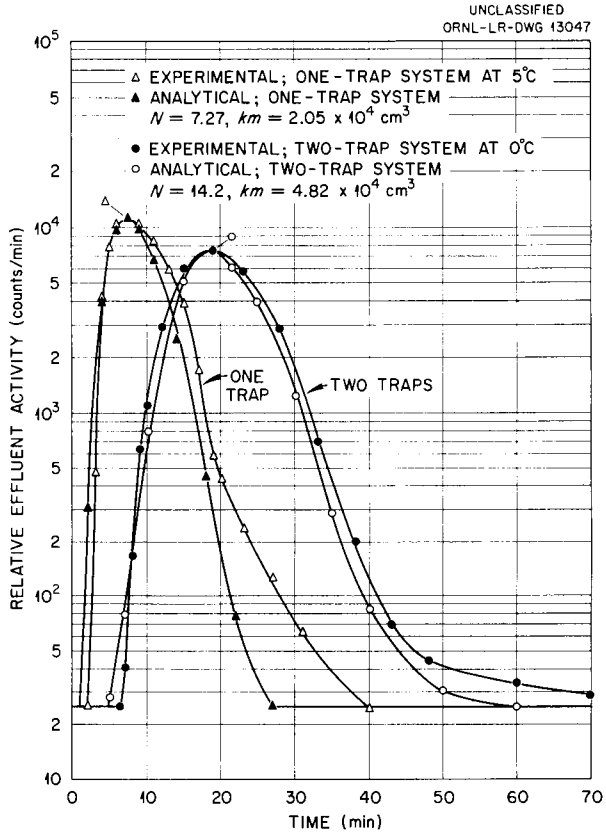

Fig. 22. Holdup of Radiokrypton in Charcoal Traps – N_2 Purge.

Figures 26 and 27 show the same data as are given in Figs. 21, 23, and 24 but with the curves plotted together for comparison. The time to reach maximum activity and the height and duration of the peaks are clearly indicated as a function of temperature.

A theoretical analysis of the adsorption process in charcoal traps has been made by making use of a number of theoretical charcoal-filled chambers, N, connected in series, which are equivalent in volume to the total volume of the trap. This is similar to the continuous-dilution tank problem in chemical engineering and applies only to systems where dilution processes, and not diffusion or adsorption, are rate-limiting. The rate of removal of radiokrypton in each chamber is first order with respect to its partial pressure and, therefore, its concentration in that chamber; that is, $dP/dt = (F/km)P$.

The N differential equations of this type for the N chambers are solved simultaneously. The general equation for the Nth chamber is:

$$(1) \quad P_n = \frac{N^N A F^{(N-1)} t^{(N-1)}}{(N-1)!\,(km)^N} \epsilon^{-NFt/km} ,$$

where

P_n = partial pressure of radiokrypton (atm),
A = amount of radiokrypton injected into first theoretical chamber (cc-atm),
N = number of theoretical chambers,
F = flow rate of purge gas (cc/min),
t = time after injection of pulse (min),
k = slope of the linear isotherm $x/m = kp$ for radiokrypton in the mixture of inert purge gas and radiokrypton $\left[\frac{\text{cc (STP)}}{\text{g·atm}}\right]$,

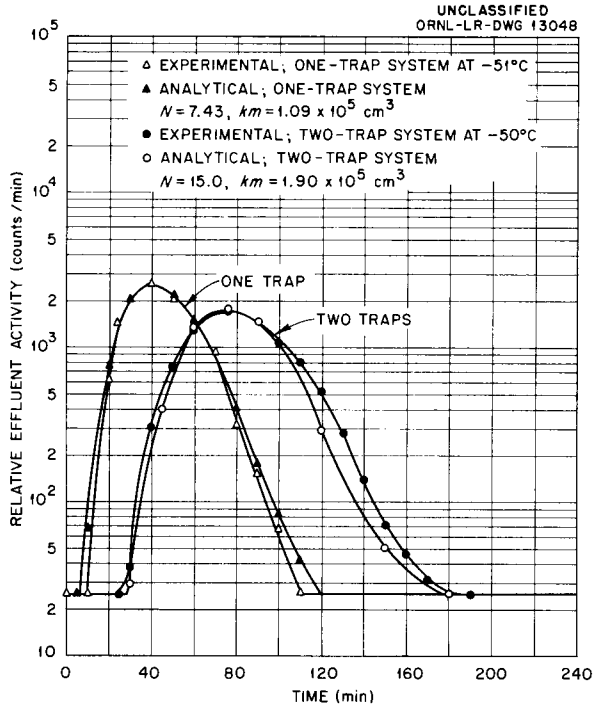

Fig. 23. Holdup of Radiokrypton in Charcoal Traps – N_2 Purge.

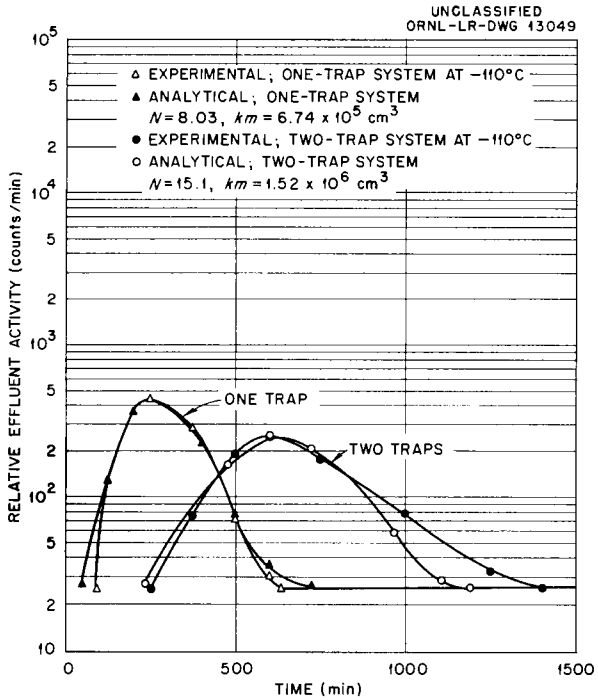

Fig. 24. Holdup of Radiokrypton in Charcoal Traps – N_2 Purge.

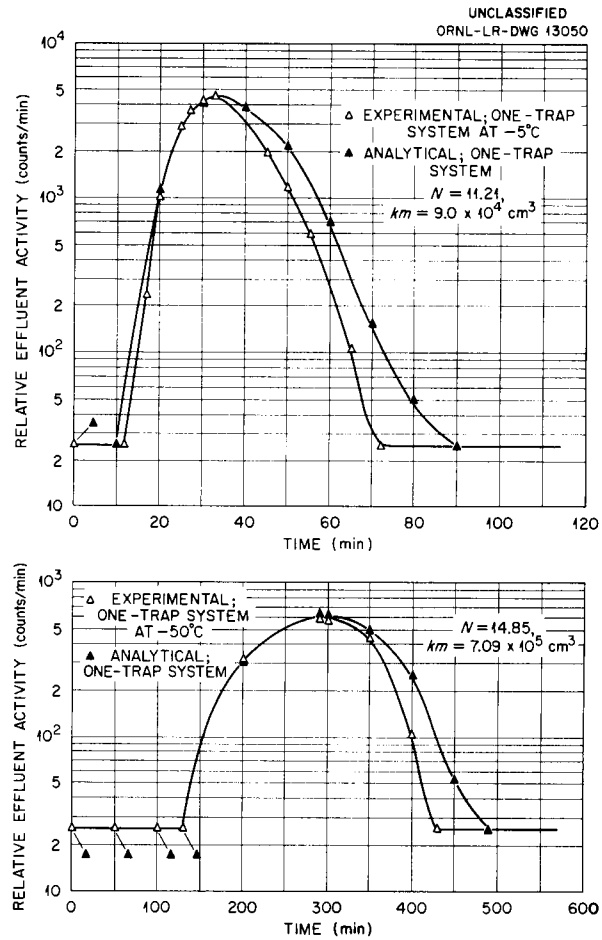

Fig. 25. Holdup of Radiokrypton in Charcoal Traps – Helium Purge.

in which

m = amount of adsorbent (charcoal) in trap (g),

x = amount of gas (radiokrypton) adsorbed isothermally $\left[\frac{\text{cc (STP)}}{\text{g}}\right]$;

km is a measure of the adsorptive capacity of the charcoal trap for radiokrypton in the presence of purge gas at the given temperature.

Parameters km and N are chosen to fit this equation to the experimental data shown in Figs. 21–24, and the resulting analytical data are plotted on the same figures. The deviations between corresponding curves are within experimental error. Figure 28 shows these parameters for various temperatures with nitrogen purge gas. It appears that the number of theoretical chambers N is a characteristic of the geometry of the charcoal

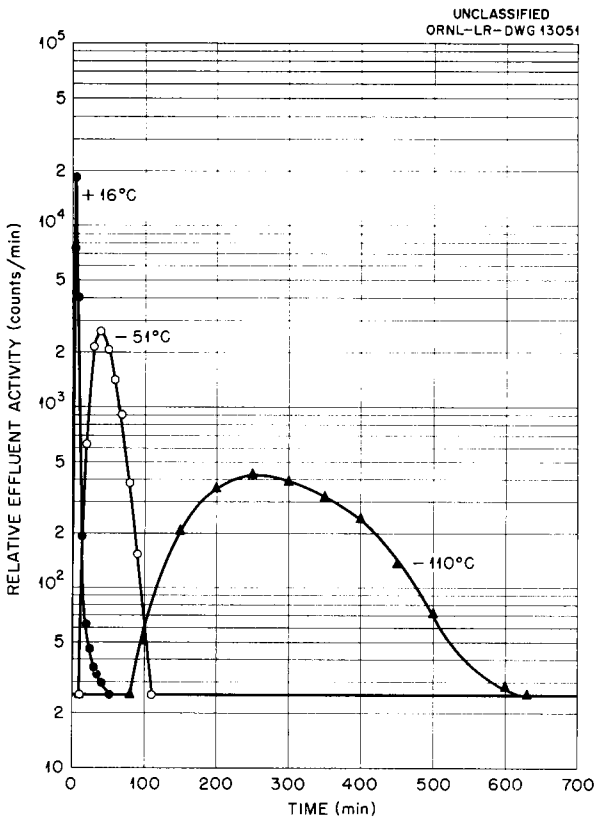

Fig. 26. Comparison of Holdup of Radiokrypton in Charcoal Traps at Various Temperatures – One Trap; N_2 Purge.

trap, since N does not vary for the different temperatures studied. This should be true if the model used to derive the expression for the curve has physical significance. For two traps in series, N is twice as large as for one trap, indicating that N may be a first-order function of the length of the trap divided by the diameter.

Figure 28 indicates that km and, therefore, k increase exponentially as $1/T$ increases (decreasing temperature), since the curves are for constant charcoal mass m. If km, the parameter obtained from holdup data by using Eq. 1, is indeed the slope of the linear isotherm multiplied by the amount of charcoal, this straight-line relationship should exist. It therefore appears that the parameter is proportional to the slope of the isotherm. Whether or not the proportionality factor is unity has not yet been established.

From Eq. 1, the time, t_{max}, to reach maximum partial pressure of radiokrypton in effluent purge gas can be derived:

$$t_{max} = \frac{(N-1)\,km}{NF} \,. \tag{2}$$

The maximum partial pressure, P_{max}, can then be obtained from Eq. 1:

$$P_{max} = \frac{N(N-1)^{N-1}\,A}{(N-1)!\,km}\, e^{-(N-1)} \,. \tag{3}$$

In Eq. 2 the time to peak depends on km and only very slightly on N. All traps with the same amount of charcoal, m, at the same temperature should have the same time to peak regardless of shape of trap. This is consistent with the data of Guss.[5] The height of the activity curve depends more on N in Eq. 3 than on km. A long thin trap would give a high narrow peak, and a short, large-diameter trap would give a broad peak with low maximum concentration.

Work is in progress to determine the relationship between N and trap shape. Further studies are planned on traps under other conditions. The results should provide engineering data for trap design and may confirm further the theoretical relationship given above.

LITR VERTICAL LOOP

W. R. Willis — D. E. Guss
M. F. Osborne — R. Shields
H. E. Robertson — W. E. Browning

Fabrication and assembly and preirradiation testing of a new vertical loop for circulating fused salt was completed. This loop is essentially the same as the one[6] which was operated in the LITR for 25 hr. Some changes were made as a result of experience with the first loop. The brush-type motor has been replaced by a three-phase induction motor whose speed is regulated by use of a variable-frequency power supply. The tip of the loop extends more than 4½ in. below the position of maximum flux in the reactor in order to obtain a greater ΔT.

The loop is to be operated in the LITR beginning in April 1956.

[5] D. E. Guss, *Solid State Semiann. Prog. Rep. Aug. 31, 1955*, ORNL-1944, p 18.

[6] W. R. Willis *et al.*, *Solid State Semiann. Prog. Rep. Aug. 31, 1955*, ORNL-1944, p 16.

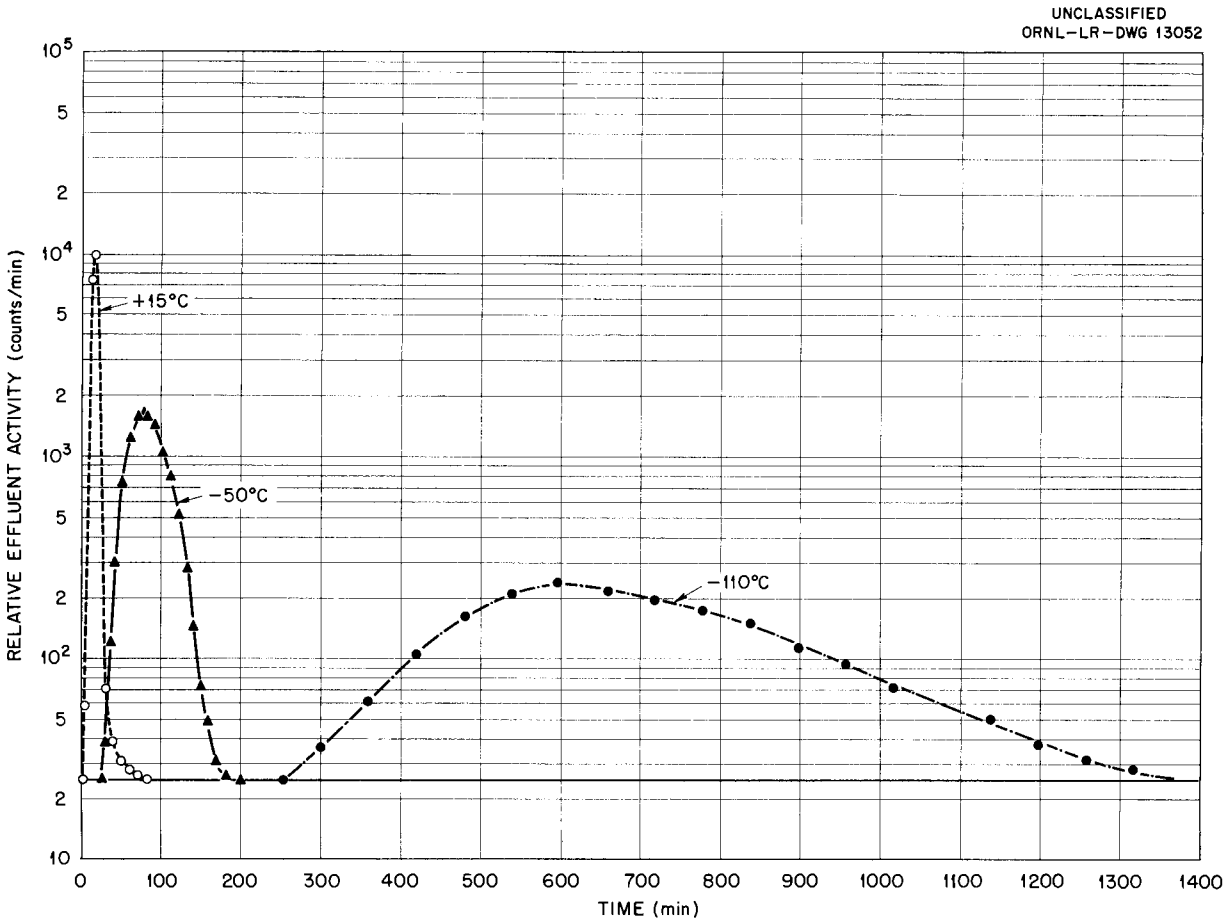

Fig. 27. Comparison of Holdup of Radiokrypton in Charcoal Traps at Various Temperatures – Two Traps; N_2 Purge.

ART OFF-GAS ANALYSIS

W. E. Browning

Design conditions for the gamma-ray spectrometer for the ART off-gas system have been provided to the ART project. Four scintillation detectors will be used, one each at the inlets and outlets of the charcoal traps in the off-gas lines from both the fuel system and the cell which encloses the reactor. Provision will be made for moving the shielded detector up to 10 ft from the most active off-gas sampling tube under normal conditions, and farther if necessary. A four-channel scintillation spectrometer will be used to monitor the detectors.

FLUX MEASUREMENTS

Inconel as a Thermal-Flux Monitor

D. E. Guss

A study is currently in progress to determine the feasibility of using Inconel as a thermal-flux monitor in the vertical in-pile loop and static-corrosion capsule programs. The advantages are twofold; first, the use of Inconel as its own monitor obviates the necessity of adding thermal-flux monitors per se to the experimental rig; and second, Inconel has the proper activation and physical properties, whereas the cobalt monitors currently available either become too radioactive during

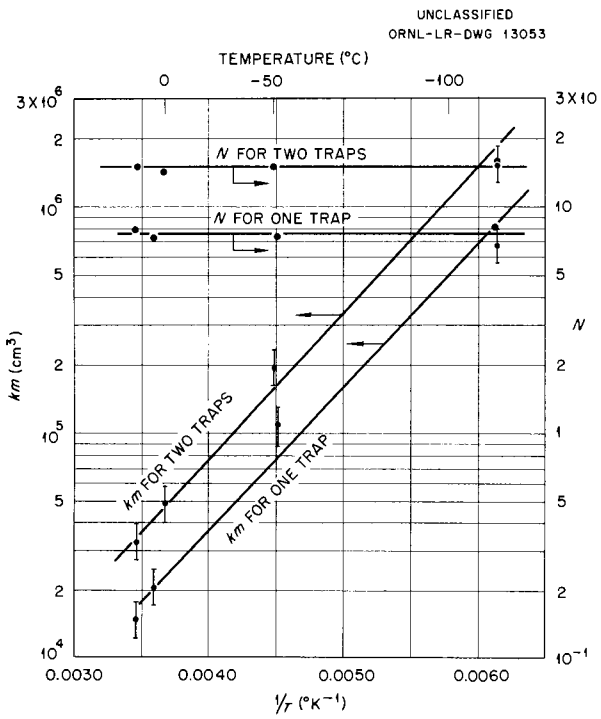

Fig. 28. Number of Theoretical Chambers, N, and Adsorptive Trap Capacity, km, vs Temperature.

long-term irradiations, melt at the high temperatures necessary to the experiments, or require extensive activation analysis before use.

There are two constituents of Inconel which can be used for flux monitoring: cobalt (~0.14% in Inconel) and chromium (~15.5% in Inconel). Cobalt has a disadvantage in that it must be chemically separated from the Inconel after irradiation to remove the Fe^{59} activity, which has gamma rays of 1.1 and 1.3 Mev. Since cobalt is present in such small quantities, there was, at first, some doubt about its homogeneity, but activation analysis of several pieces of Inconel stock shows that, within a given batch of Inconel, the cobalt is homogeneous enough for monitoring purposes.

Chromium-50, 4.4% naturally abundant, is transformed by neutron capture to Cr^{51}, with a thermal cross section of about 15 barns. Chromium-51 has a half life of 26.5 days and decays by K capture with an associated 0.32-Mev gamma ray in about 9% of the disintegrations. A gamma-spectrometer scan of irradiated Inconel has shown that the Cr^{51} peak is large enough to provide a good value for the chromium activity by area analysis. The cadmium ratio of chromium in the lattice of the LITR was measured to be 29, which is consistent with the value to be expected for a $1/v$ absorber. The cross section is known to be about 15 barns, but a more accurate measurement must be made.

The disadvantage in using chromium for long-term irradiations is its relatively short half life. This limits the time of irradiation for which chromium could be effectively used as a flux monitor to one or two months, after which time it is too far up on the saturation curve to be effective as an integrated-flux monitor.

In conclusion, the cobalt has the advantage of a long half life but must be chemically separated from the Inconel, whereas the chromium, although it requires no separation, has the disadvantage of a short half life. For irradiations up to about two months duration, the chromium would be better for monitoring the thermal flux because of the ease with which its activity can be determined. For longer irradiations, however, the cobalt would give a more accurate value for the thermal flux.

The flux near the tip of the MTR loop (ORNL-20-3) was measured by cobalt monitor foils which were attached to the fuel tube wall at the positions shown in Fig. 29. The integrated thermal flux and average thermal flux for each position are given in Table 2.

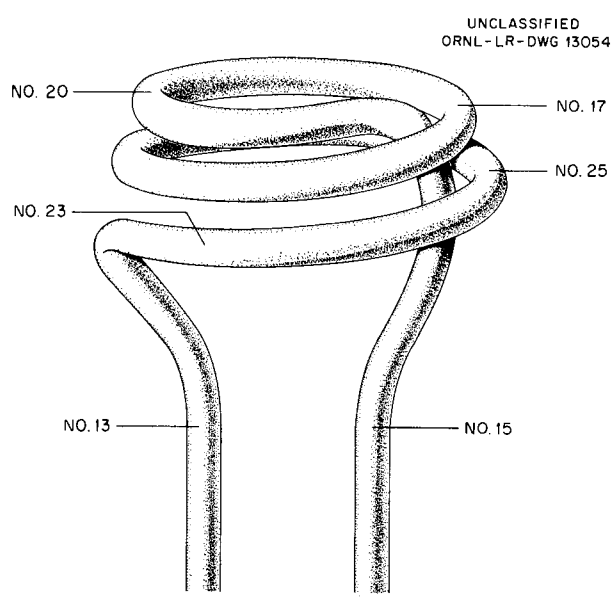

Fig. 29. Position of Monitor Foils in MTR Loop.

TABLE 2. FLUX DISTRIBUTION FOR MTR LOOP

Foil No.	Integrated Flux (neutrons/cm^2 $\times 10^{19}$)	Average Flux (neutrons·cm^{-2}·sec^{-1} $\times 10^{13}$)
13	Lost	
15	3.85	4.06
17	7.08	7.46
20	8.20	8.64
23	5.90	6.22
25	4.18	4.41

Fast-Flux Measurements

J. F. Krause

Two flux traverses have been run in hole 19 of the Graphite Reactor. The first used the threshold reaction $S^{32}(n,p)P^{32}$ for the flux measurement above 2.9 Mev; the second used the $Co^{59}(n,\gamma)Co^{60}$ reaction to obtain the thermal flux. Each traverse is fairly constant from the center of the reactor to a point 30 in. from the center. Over this range the flux as measured is approximately 2.5×10^3 neutrons·cm^{-2}·sec^{-1}·watt^{-1} (above 2.9 Mev) and 2.4×10^5 neutrons·cm^{-2}·sec^{-1}·watt^{-1} (thermal). All measurements were made in the $\frac{1}{8}$-in.-wall aluminum specimen cans ordinarily used in hole 19. These cans were surrounded by $\frac{3}{16}$ in. of flowing water, which acts as the carrier as well as the coolant. Previous measurements in hole 19 were made during the irradiation of specific materials which may have altered the flux. Similar measurements have been started in facility HB-3 of the LITR, where the stress-corrosion tests are being run on Inconel with fluoride fuel.

CHEMICAL EFFECTS OF NUCLEAR REACTIONS

M. T. Robinson

EFFECTS OF THE FISSION PRODUCTS ON THE PROPERTIES OF ANP FLUORIDE FUELS

M. T. Robinson J. F. Krause[1]

In uranium-containing systems like the fused-fluoride ANP fuels, three different types of radiation effects may be distinguished:

1. radiation damage due to bombardment of the medium with high-energy particles and with electromagnetic radiation,
2. bulk thermal effects due to the large amount of energy dissipated in the medium as heat,
3. chemical effects due to replacement of uranium by a mixture of more than 30 other elements.

The fluoride fuels consist largely of ions, some simple (e.g., Na^+ and F^-) and some complex (e.g., ZrF_5^-, UF_5^-). In all likelihood the bonding in the complex ions is largely ionic. For example, on the basis of the method of Pauling,[2] a Zr-F bond is found to be about 75% ionic. In such a system, radiation-damage effects should be very small, since there are neither covalent bonds to sever (as in H_2O or organic compounds) nor a solid lattice to disrupt. Bulk thermal effects, while providing a great deal of difficulty in the interpretation of continuous in-pile measurements, are not particularly important in corrosion studies where the fuel-metal interface temperature is controlled and are of even less significance in turbulently flowing systems. It is the purpose of this report to present the results of some calculations on the effects of fission products on the properties of the fluoride fuels.

A series of calculations has been performed[3] which makes available, as functions of time, the yields of the various chemical elements in thermal-neutron fission of U^{235}. These results may be used to calculate the *average valency* of the fission-product mixture. Before doing this, it is necessary to discuss briefly the likely chemical form which each element will adopt in a high-temperature fluoride liquid.

Group 0. – Krypton and xenon will occur only in the elementary form.

Groups IA, IIA, IIIB, and IVB. – These elements will adopt their usual group valencies:

+1: Rb, Cs

+2: Sr, Ba

+3: Y, La, Ce, Pr, Nd, Pm, Sm, Eu, Gd, Tb, Dy

+4: Zr

There is a possibility that, if the medium becomes sufficiently oxidizing, some Ce(IV) will be present, particularly since it may be stabilized by formation of some complex ion like CeF_5^-. Similarly, in a strongly reducing medium, some Eu(II) is to be expected. However, the low yield of europium makes this a relatively unimportant point.

The Transition Metals. – The elements beyond zirconium in the periodic table are all relatively noble in comparison with chromium. Accordingly, it has been observed that ruthenium and niobium deposit from fluoride fuels onto the Inconel container.[4] The sparse thermodynamic data[5] indicate that chromium will reduce germanium, arsenic, and all the metals from niobium through antimony to the elemental state. Where valencies are required for these metals, the following values have been chosen:

+1: Ag, In

+2: Ge, Tc, Pd, Cd, Sn

+3: As, Nb, Mo, Ru, Rh, Sb

These are, in general, the lowest known valencies which have been reported for each element. Fluorides exhibiting these valencies are not known in every case.

Groups VIA and VIIA. – The valencies to be expected for Se, Te, Br, and I will depend strongly

[1] On loan from Pratt & Whitney Aircraft.

[2] L. Pauling, *Nature of the Chemical Bond*, 2d ed., p 70, Cornell University Press, Ithaca, 1940.

[3] M. T. Robinson and J. F. Krause, *Solid State Semiann. Prog. Rep. Feb. 29, 1956* (in preparation).

[4] M. T. Robinson, T. H. Handley, and W. A. Brooksbank, *Solid State Semiann. Prog. Rep. Aug. 31, 1955*, ORNL-1944, p 17–18.

[5] L. Brewer *et al.*, "The Thermodynamic Properties of the Halides," in *Chemistry and Metallurgy of Miscellaneous Materials; Thermodynamics* (ed. by L. L. Quill), NNES IV-19B, p 76–192, McGraw-Hill, New York, 1950; W. M. Latimer, *Oxidation Potentials*, Prentice Hall, New York, 1938.

on conditions in the fluoride melt. Under moderate reducing conditions the expected states are the normal anions:

−2: Se, Te

−1: Br, I

If the conditions are mildly oxidizing, the elemental forms are to be expected (valency 0). Under stronger oxidizing conditions, positive valencies may be anticipated.

The average valencies of the fission-product mixture under various conditions are plotted in Figs. 30 and 31 as functions of irradiation time. The region above a valency of 4 represents reducing conditions, and that below represents oxidizing conditions, compared with an original uranium valency of +4. The curves marked "inert container" are based on the assumption that in capsules (Fig. 30) all krypton and xenon descendants are retained and that in reactors (Fig. 31) the descendants of rare-gas isotopes of half life greater than 10 min are lost completely. The left branch of each curve, up to valency 4, is based on the elemental state of the halogens and chalcogens. The right branch is based on the anionic forms of these elements. In the intermediate branch, the halogens and chalcogens are progressively reduced from the elemental forms to the normal anions.

[redacted]

ORNL-LR-DWG 11720

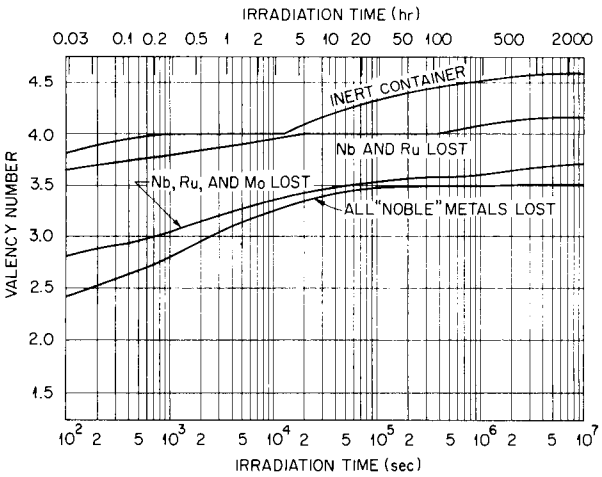

Fig. 30. Average Fission-Product Valency in Irradiated Fused-Fluoride Capsules.

[redacted]

ORNL-LR-DWG 11719

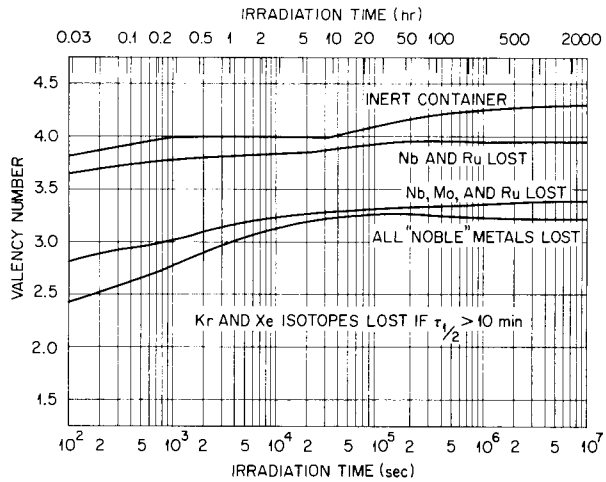

Fig. 31. Average Fission-Product Valency in Circulating-Fuel Reactors.

The curves marked "Nb and Ru lost" were plotted on the assumption that these two metals deposit on the container walls as elements. Where the valency is below 4, the halogens and chalcogens are taken as the elements; where it is above 4, these nonmetals are taken as the normal anions. The great importance of molybdenum in determining the average valency of the fission products may be seen from the remaining curves, which show the average fission-product valency for loss of Nb, Mo, and Ru and for loss of all the "noble" transition metals.

In Figs. 32 and 33 are presented curves showing the excess "fluorine" present in fluoride fuels as a result of the low average valency of the fission products. The right ordinate is marked with the concentration of excess Cr^{++} ion required to balance the excess oxidizing power of the fuel. It is very evident from these curves that a substantial increase in the corrosive attack of the fuel on the container may be expected under irradiation, as compared with the ordinary thermal corrosion, the effect becoming more serious as the fission rate (w/cc) is increased. This results from the instability, in contact with Inconel, of ions of molybdenum and ruthenium. Other things being equal, the effect is expected to be more serious in systems in which the fission gases are removed with high efficiency than in systems where they are retained (cf. Figs. 30 and 31).

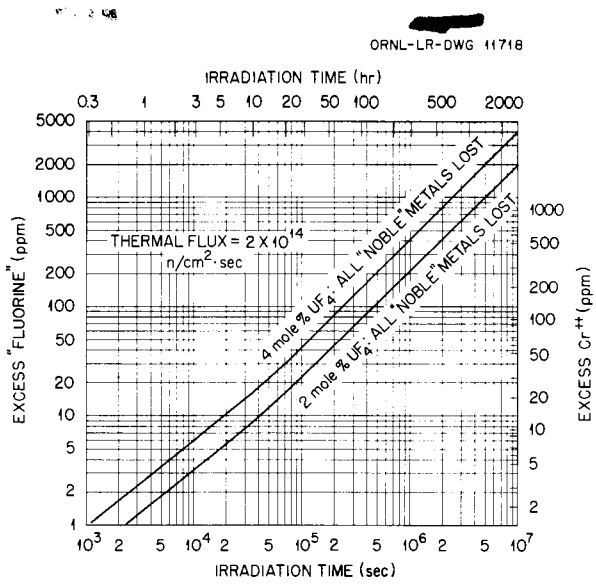

Fig. 32. Excess "Fluorine" in Irradiated Capsules in the MTR.

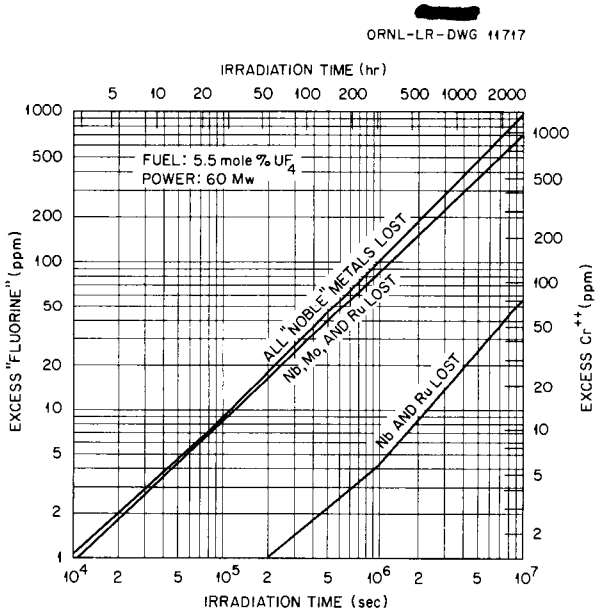

Fig. 33. Excess "Fluorine" in the ART Reactor Fuel.

Contrary to these theoretical predictions, corrosion in irradiated fluoride systems has never been observed to be increased over what would be anticipated from unirradiated controls. No increased penetration of the irradiated metal is observed. The container-metal content of the irradiated fuels is generally much the same as, or even less than, the amounts found in unirradiated controls. It is evident that the excess oxidizing power of the irradiated fuel, which has been expressed here in terms of "fluorine," is tolerated without increased attack on the container. The following are some of the possible ways of absorbing this oxidizing power:

MoF_6. – Only a small part of the total molybdenum need remain in solution as Mo(VI) to absorb the entire excess oxidizing power. However, the necessary amount of molybdenum is believed to be far greater than the fuels will tolerate.

Fluorides of Se, Te, Br, and I. – These elements all form a series of volatile fluorides, for example, SeF_6, TeF_6, BrF_3, IF_5. A portion, perhaps two-thirds, of the oxidizing power of the fuel could be absorbed in such compounds. These compounds, like MoF_6, are strong oxidizing agents, and their existence in the fuels can be only transitory, unless they escape as gases. The results of capsule irradiations argue against this possibility.

CeF_4. – As was suggested above, at least some of the excess oxidizing power might well be absorbed as Ce(IV), in the form of a complex ion, such as CeF_5^-. Such an ion would be present in comparatively small amounts and might well serve as a "tracer" for the very similar ZrF_5^- ion. The yield of cerium is such that about one-fourth the oxidizing power could be thus absorbed in systems where the rare gases were lost and almost one-half in systems where they were retained.

UF_5. – Another way of absorbing the oxidizing power of the fuel would be by the oxidation of U(IV) to U(V):

$$UF_5^- + F = UF_5 + F^-$$

In the fuel of the ART, this would require oxidation of up to 2% of the uranium after 500 hr of operation.

Solid Fluorides. – It is perhaps possible that the "noble" metal deposit is not metallic but contains polymerized subfluorides, such as $(MoF)_x$. These materials would reduce the oxidizing power of the fuel about half in the reactor case.

No one of the above suggestions accounts for all the excess "fluorine" released by the fissioning uranium. In every case a substantial oxidizing power remains. The fact that this causes no increase in corrosion argues convincingly that the

deposited fission-product layer effectively inhibits corrosion of Inconel by the fuel.

Some comments may now be made on the effect of the fission-product mixture on the physical properties of the fuel. The well-known theory of Frenkel[6] concerning the viscosity and electrical conductivity of fused salts is a useful starting point. The viscosities of fused salts are determined by the larger ions present, which in the case of the fuels being considered are species such as UF_5^- and ZrF_5^-. The fission process decreases the number of these large ions by replacing them with the small ions Rb^+, Ba^{++}, La^{+++}, etc., none of which are likely to be complexed. Therefore a small *decrease* is expected in the viscosity of the fuel with increasing time of irradiation. This decrease in viscosity will be exceedingly small, however, because of the relative rarity of UF_5^- ions (about one complex anion in four), the low burnups envisioned in aircraft reactors, and the high fission yield of zirconium. There will be a similar small *increase* in the electrical conductivity of the fuels. The effect of the fission products on thermal conductivity cannot be estimated because of the lack of a suitable theory, but any effect will certainly be very small. The *molar* heat capacity of the fuel may be taken as independent of composition, to a first approximation. The only effect of fission will be to increase slightly the effective molecular weight of the fuel through loss of noble gases, molybdenum, ruthenium, etc. Thus the specific heat of the fuel will decrease very slightly as irradiation proceeds.

In conclusion, the only important effect of the fission process on the properties of the fused fluoride fuels is on corrosion. Theory predicts a substantial increase in the corrosion rate as irradiation continues. The absence of such an effect in all experiments to date leads to the suggestion that deposition of niobium, ruthenium, and (presumably) molybdenum on the container effectively inhibits the attack of the fuel on Inconel.

USE OF NATURAL LITHIUM IN IN-PILE CORROSION TESTING OF ANP FLUORIDE FUELS

M. T. Robinson J. F. Krause

The chemical effects of the fission products on corrosion of Inconel by fuels in the $NaF\text{-}ZrF_4\text{-}UF_4$ system have been discussed above. An additional problem encountered in the $NaF\text{-}KF\text{-}LiF\text{-}UF_4$ system arises from the nuclear reaction

$$^6Li^+ + n \longrightarrow {}^4He + T^+$$

In Fig. 34 is shown the concentration of tritium ion in fuel composition 107 (natural lithium) as a function of time. The concentration is expressed as the pT of the solution:

$$pT = -\log \text{(gram-ions of } T^+ \text{ per liter of solution)} .$$

On the right ordinate is shown the equivalent concentration of chromium in the fuel, which would be produced by the reaction

$$2T^+_{(soln)} + Cr_{(Inconel)} \longrightarrow Cr^{++}_{(soln)} + T_{2(gas)}$$

It is evident that large increases in corrosion will occur in such a fuel, especially in capsule irradiations in the MTR, unless at least part of the Li^6 is removed from the fuel.

Because of the large neutron-absorption cross sections of fuels containing natural lithium, there will be substantial decreases in the effective neutron flux in such materials, as compared with similar ones using pure Li^7. Because of this and also because of the large dilution factors generally encountered in in-pile loops, the chemical effects of tritium production will be much less serious than in capsules. Nevertheless, in order to obtain satisfactorily high fission rates with present loop designs, removal of some of the Li^6 will be required.

In order to keep that portion of the corrosion attributable to tritium below 100 ppm chromium in 300 hr, it is necessary that any lithium employed in MTR capsule irradiations of fuel 107 contain less than 0.2% Li^6. In loop experiments on this fuel, up to 1% Li^6 can be tolerated without reducing the fission power at the tip of the loop below 1000 w/cc. This amount of Li^6 will also restrict tritium corrosion to less than 100 ppm of extra chromium per 300 hr.

There seems to be no reason to expect the apparent fission-product protection of Inconel found in $NaF\text{-}ZrF_4\text{-}UF_4$ fuels to reduce the attack of T^+ on the metal surface. The exact distribution of tritium among the various species, T^+, TF_2^-, TF (soln), and TF (gas), is believed to be unimportant.

[6] J. Frenkel, *Kinetic Theory of Liquids*, p 439–445, The Clarendon Press, Oxford, 1946.

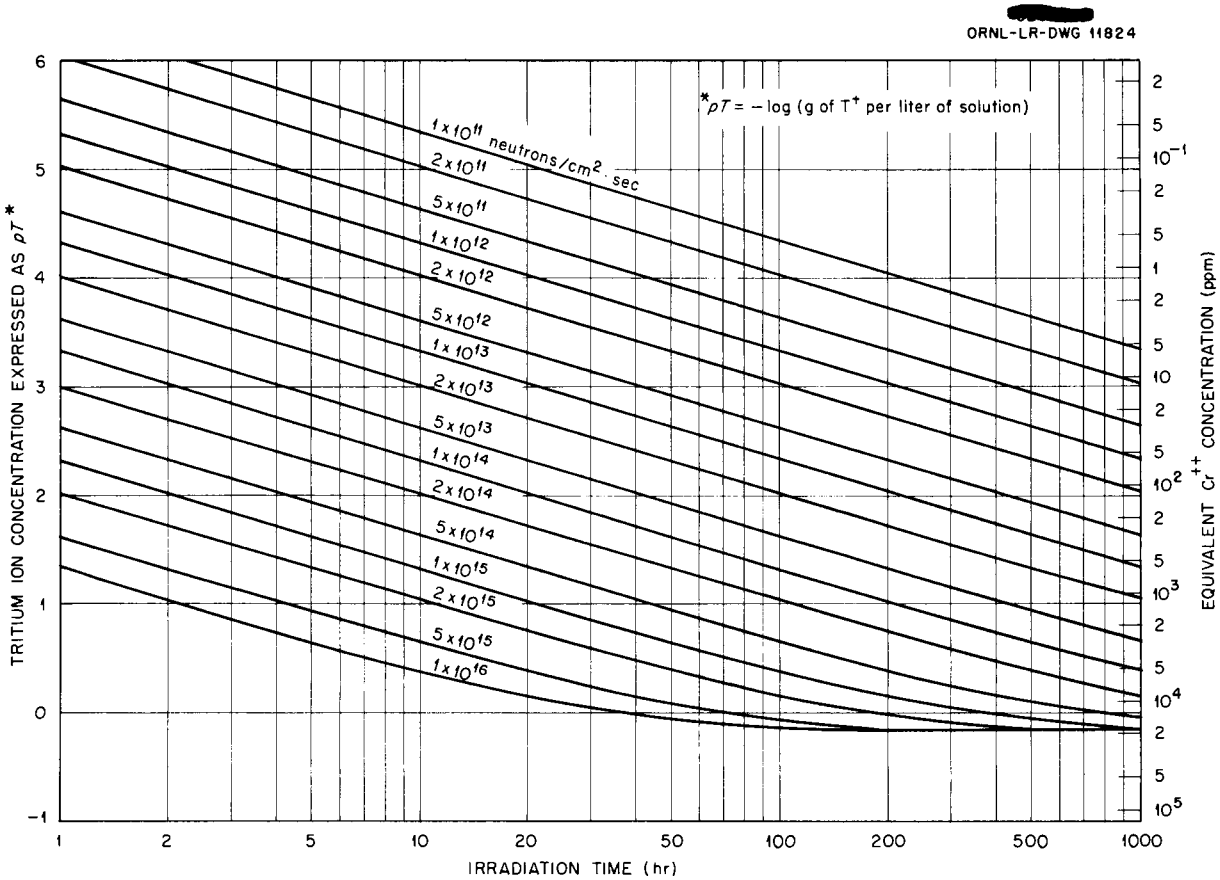

Fig. 34. Production of Tritium in Fluoride Fuel 107 at Various Thermal-Neutron Fluxes as a Function of Time.

SPECIAL PROJECTS

HOT METALLOGRAPHY

M. J. Feldman C. Ellis
A. E. Richt R. N. Ramsey
W. B. Parsley E. J. Manthos
E. D. Sims

Examination of two fuel elements for the GE-ANP Division has been completed and reported.[1] Irradiation of both elements had been terminated by fission-fragment release into the cooling air stream. Examination of the GE-ANP-3E fuel element revealed a highly oxidized area immediately downstream from the position where a controlling thermocouple had been located. Failure of the element was therefore thought to be caused by localized overheating of the element as a result of improper thermocouple positioning. Examination of the GE-ANP-3W fuel element revealed the presence of three small blistered areas. Metallographic examination revealed failure of the clad in two locations at the extremities of the blister. The actual mechanism which caused the blistering is unknown. Metallographic evidence tends to indicate that blistering was caused by fission-gas formation, with the resulting localized stress and higher operational temperatures resulting in failure of the clad.

Work has continued on specimens from the Homogeneous Reactor Project. Examination of corrosion coupons from in-pile loop FF has been completed. Publication of results will be made after examination of stress-corrosion samples from this loop is completed. Components of HRP in-pile loop EE have also been examined. Again, publication of results is awaiting examination of corrosion coupons from this loop.

Examination of samples taken from the North Carolina State University Reactor revealed localized corrosive penetration of the core tank at a position near the liquid-vapor interface area. The physical characteristics of the corroded area are quite similar to those that occur in the vapor phase when the fuel solution is high in chloride content. Analysis of the fuel did reveal chloride to be present. Examination of sections of tubing from the cooling coil revealed evidence of stress corrosion caused by the high chloride content of the tap water used as a cooling medium. Examination of additional sections from both the cooling coil and the core tank will be made to determine if failure of the cooling-coil tubing was responsible for the introduction of chloride to the fuel solution. Results of the examination will be published upon completion of the examination of these additional sections.

The loop-sectioning project, at the GE-ANP site in Idaho Falls, has been completed. Three carriers containing the different sections of the loop have been received in Oak Ridge. The first carrier received contained the nose coil and two 14-in.-long pairs of fuel tube from behind the nose. The nose coil was stripped of foil, thermocouples, Calrods, and insulation. Five of the six cobalt foils were found and removed; D. E. Guss, of the Solid State Division, received the foils for analysis. Figure 35 shows the stripped nose coil, along with part of the heat-exchanger assembly. The nose coil was then sectioned on a hack saw and melted out in an argon atmosphere at a temperature of approximately 650°C. C. C. Webster of the Solid State Division melted the fuel out of the two pairs of 14-in. fuel tubes. Thirty-five metallographic samples were obtained from the nose coil, heat exchanger, bellows, and the fuel tubes; location of these specimens is shown in Fig. 36 and in Table 3.

All the specimens from the nose coil have been examined microscopically in the as-polished condition. In the unetched condition no evidence of attack was seen. Wall thickness measurements were taken on four samples from the coil and on the original tubing. Statistical variations in wall thickness of the original tubing, and variations due to bending of the tubing were established. Measurements taken on the four samples from the nose fell within the inherent variations in the nose. Attempts to etch these specimens either chemically or electrolytically have not been satisfactory and have resulted in what appears to be moderate intergranular attack to a depth of 1 mil; however, this may only be an etching effect and not actually corrosive attack. Figures 37–40 show the condition of samples 264 and 271 in both the as-polished and etched conditions. At the present time two etching techniques show

[1] A. E. Richt, R. N. Ramsey, and W. B. Parsley, *Metallographic Examination of GE-ANP-3E and GE-ANP-3W Fuel Plates*, ORNL CF-56-1-102 (Jan. 19, 1956).

Fig. 35. Stripped Nose Coil and Part of Heat-Exchanger Assembly.

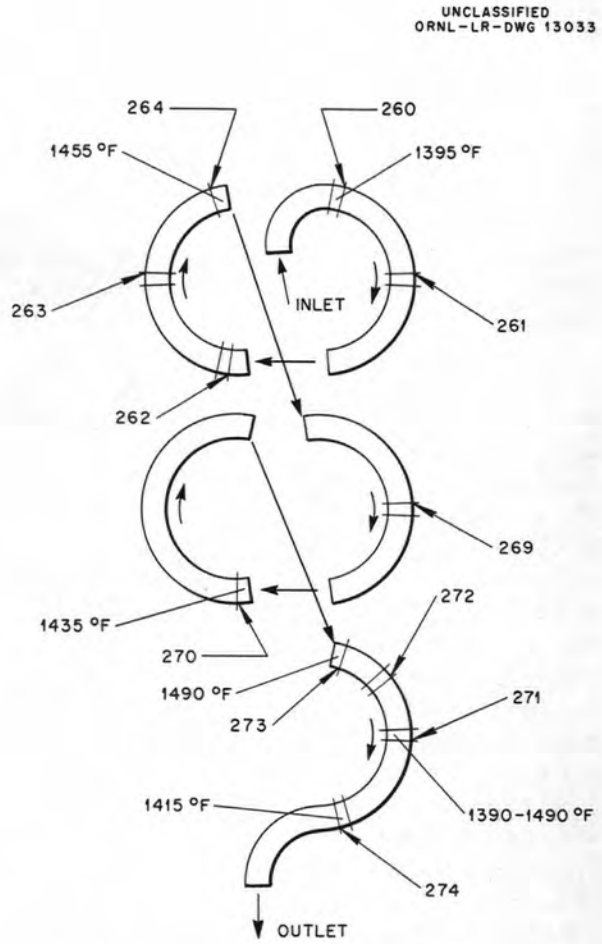

Fig. 36. Sectioning Diagram of Nose Coil of ANP Loop No. 3. (Secret with caption)

promise toward providing a more definable microstructure.

Work is anticipated on several projects:

1. The pump and two remaining sections of fuel tubes will be examined as soon as two cells are decontaminated so as to allow equipment to be serviced by personnel.

2. Two sections of fuel tube will be received by R. Shields, of the Solid State Division, for chemical analysis of the fuel. Sections of the melted-out straight fuel tubes will also be given to Shields for analysis of the tube walls.

3. Plans for sectioning of the next loop have already begun. A meeting with D. Durrill of GE

TABLE 3. METALLOGRAPHIC SAMPLE LOCATIONS FROM ANP LOOP NO. 3

Sample No.	Sample Location
280	Section of weld from heat-exchanger U-joint
281	Transverse section of bellows on heat exchanger from outlet side
283	Transverse section of bellows on heat exchanger from outlet side
284	Radial section at location of thermocouples 5, 6, and 7 on outlet side
285	Transverse section of heat-exchanger weld on outlet
286	Transverse section of helium sniffer line and fuel tube at point where helium sniffer line ends
287	Radial section at location of TC-21
288	Same as 284 except on outlet side
289	Same as 285 except on outlet side
290	Radial section at location of TC-18
291	Radial section on outlet side 10½ in. from end of helium sniffer line
295	Radial section on outlet side 15½ in. from end of helium sniffer line
296	Radial section on outlet side 20 in. from end of helium sniffer line
297	Radial section at location of TC-23 on outlet side
303	Radial section on outlet side 30 in. from end of helium sniffer line
304	Radial section on inlet side 7 in. from end of helium sniffer line
305	Radial section on inlet side 12 in. from end of helium sniffer line
306	Radial section on inlet side 17 in. from end of helium sniffer line
307	Radial section on inlet side 21 in. from end of helium sniffer line
308	Radial section on inlet side 25 in. from end of helium sniffer line
309	Radial section on inlet side 30 in. from end of helium sniffer line

and J. Burnham of the MTR was held February 7 and 8 concerning the location of the next loop-sectioning project. Plans are being made to bring the active part of loop 4 back to Oak Ridge in one section; the carrier is being built at the present time.

4. Examination of ARE components, which has come to a standstill because of the loop program, will be resumed.

Four pin-type elements irradiated by KAPL have been examined and a report has been prepared.[2] All four of the samples had split open during irradiation. The cross section of the breaks showed that the cracking had occurred where the relatively square core made its closest approach to the outside of the circular clad. Figure 41 shows the general appearance of the breaks. When examined, no corrosive penetration of the stainless clad was noted. Of interest was a definite difference in the appearance of the UO_2 after irradiation. Figure 42 shows the KAPL control photograph of the 90-mil pins before irradiation, and Fig. 43 shows the same material after irradiation. Similarly, on the 160-mil wires a definite difference was noted. Figure 44 shows the control structure and Fig. 45 shows the irradiated structure.

Examination of the last two capsules which comprise the P&W-ORNL-BMI fuel-element study was completed by the Hot Metallography Group.[3]

[2] M. J. Feldman, A. E. Richt, and E. J. Manthos, *Metallographic Analysis of KAPL Samples 3R, 6R, 18R, and 19R*, ORNL CF-56-1-20 (Jan. 4, 1956).

[3] M. J. Feldman, *Postirradiation Metallographic Examination of Pratt & Whitney Capsules 1-12 and 1-13*, ORNL CF-56-1-105 (Jan. 16, 1956).

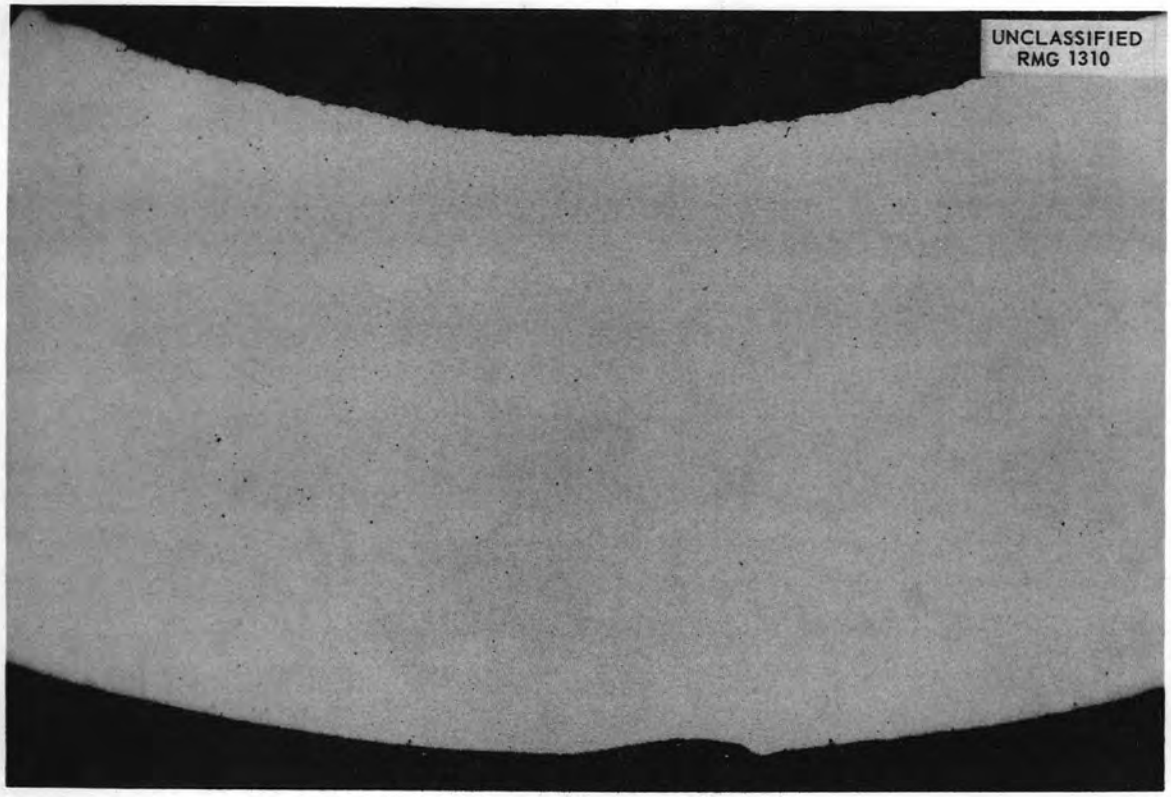

Fig. 37. Sample No. 264 – As Polished. No apparent corrosive attack. 50X. (Secret with caption)

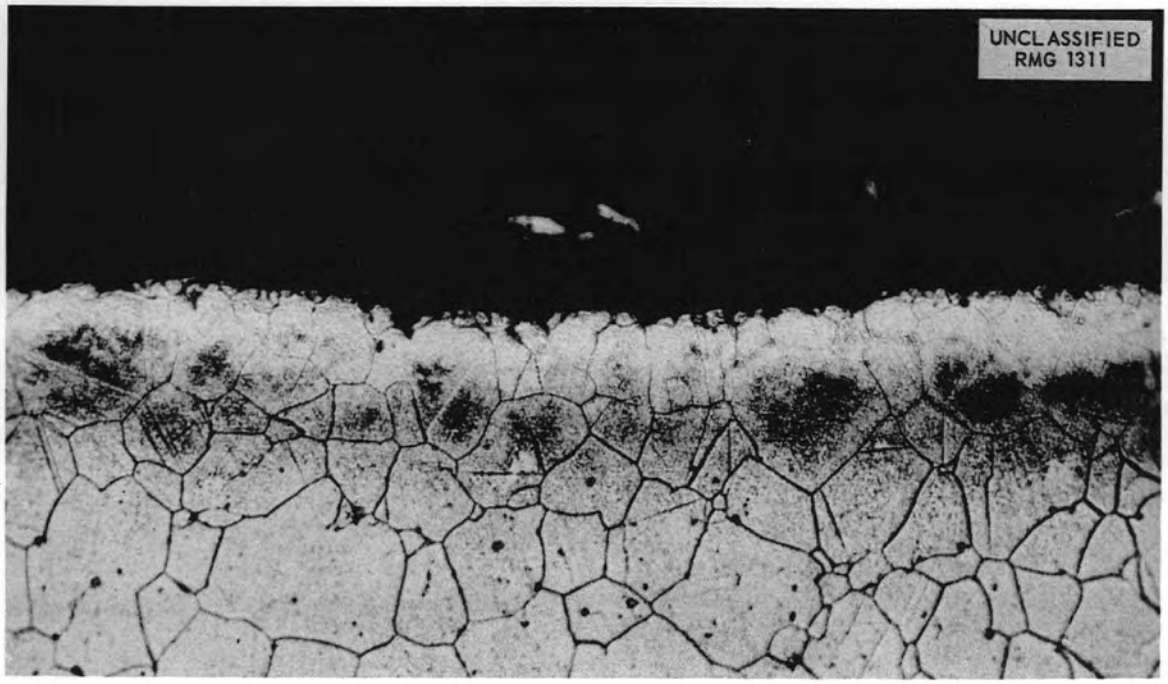

Fig. 38. Sample No. 264. Etchant: 10% H_2SO_4 (electrolytic). 250X. (Secret with caption)

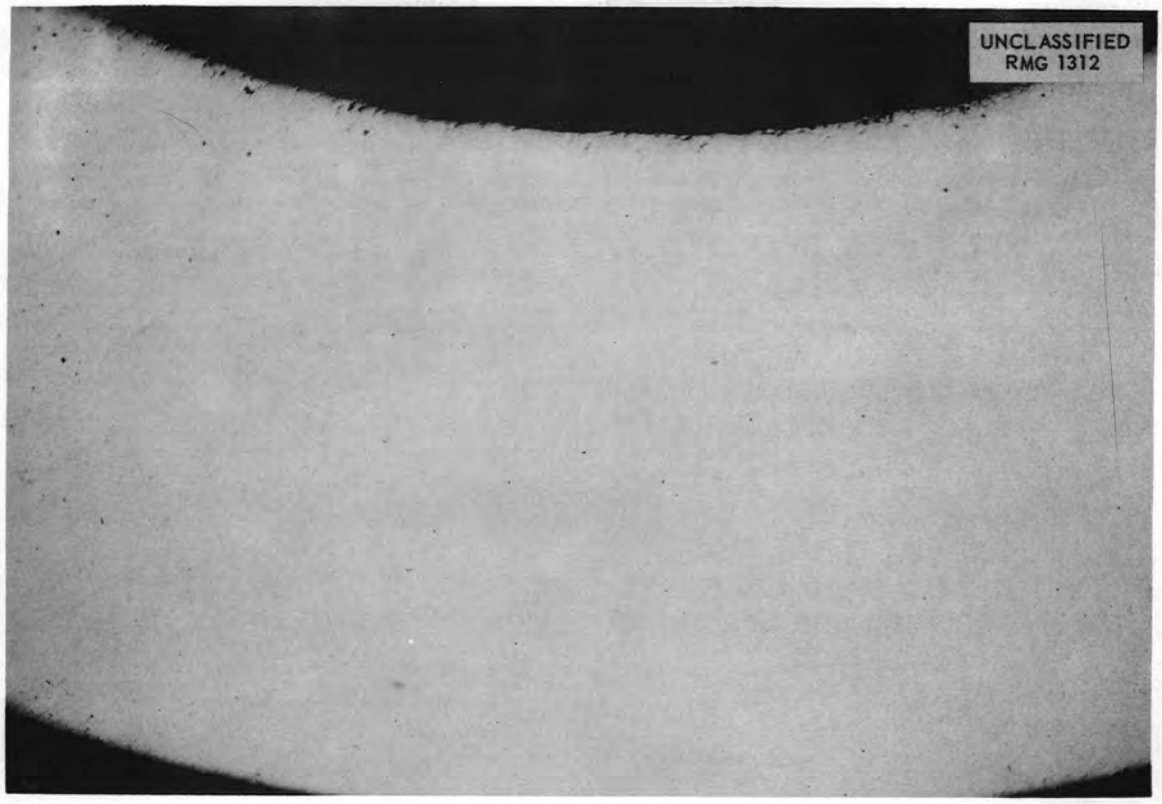

Fig. 39. Sample No. 271 – As Polished. 50X. (Secret with caption)

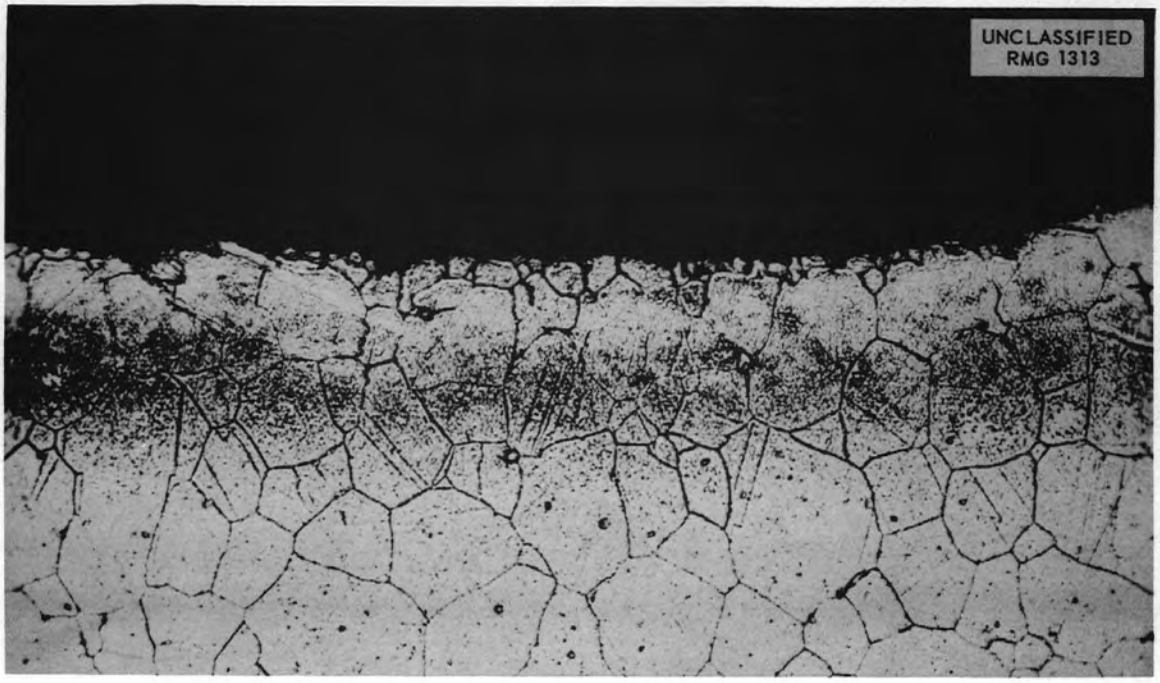

Fig. 40. Sample No. 271. Etchant: 10% H_2SO_4 (electrolytic). 250X. (Secret with caption)

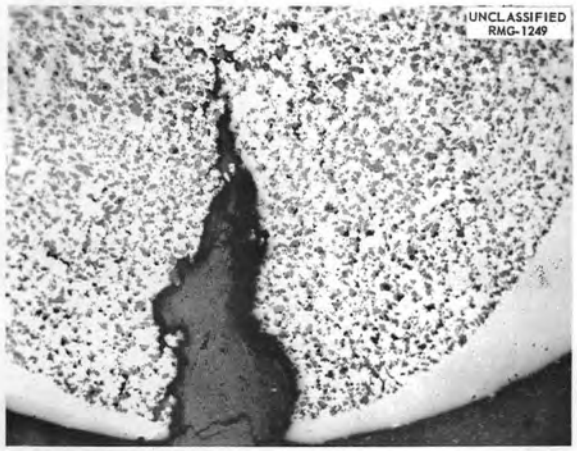

Fig. 41. KAPL Fuel Rod 19R. Fracture in cladding. 50X. Reduced 34%. (Secret with caption)

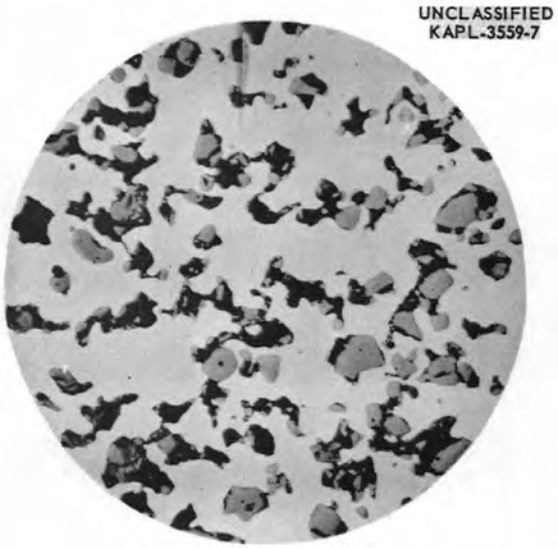

Fig. 42. Sample 15D. Appearance of UO_2 before irradiation. 500X. Reduced 8%. (Secret with caption)

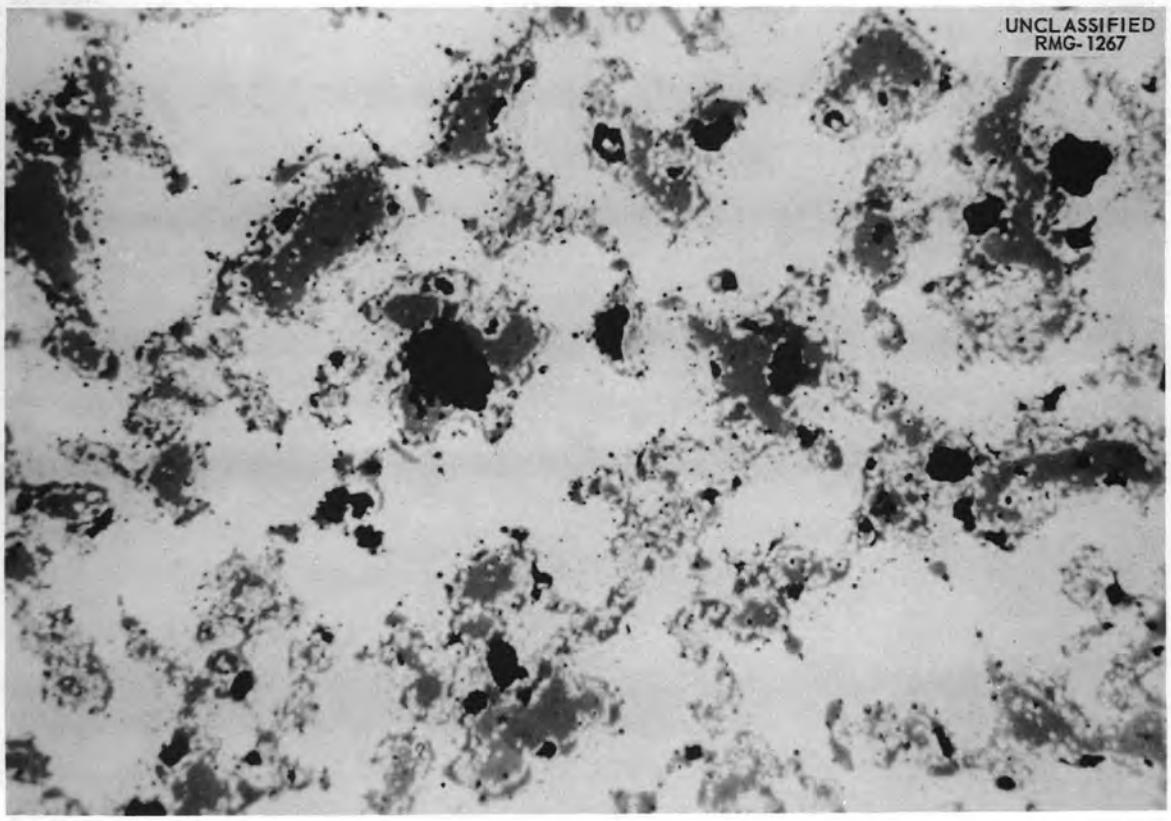

Fig. 43. Sample 6R. Appearance of UO_2 after irradiation. 1000X. (Secret with caption)

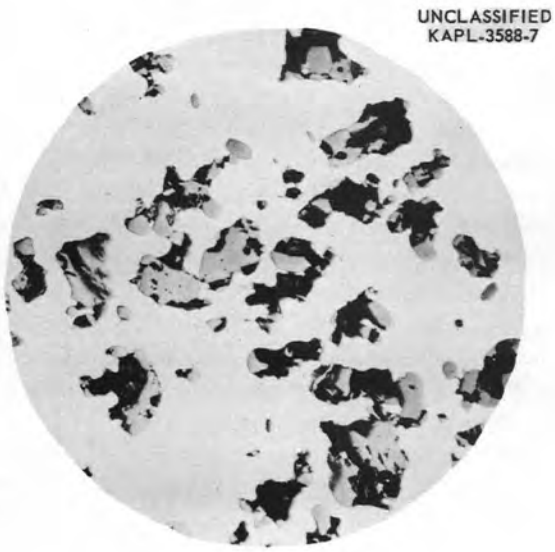

Fig. 44. Sample 21R. Appearance of UO_2 before irradiation. 500X. Reduced 8%. (Secret with caption)

Of interest in this examination was the fact that the first occurrence of blistering of elements was noted. The blistering occurred in elements of both the small (<3 μ) and the larger (15–44 μ) UO_2 particle sizes. Of the variables of operation which could have contributed to the blistering, only the variable of time had not been exceeded in an earlier experiment. While this series of experiments is not conclusive, the usual combination of temperature and burnup, which had generally been thought of as the cause of blistering, should now have the variable of time added to it.

HOT-CELL OPERATION

S. E. Dismuke M. J. Feldman E. S. Schwartz

The dismantling and analysis of HRP in-pile loop EE, discussed in a previous progress report,[4] was completed in the hot cells.[5] In addi-

[4] S. E. Dismuke, M. J. Feldman, and E. S. Schwartz, *Solid State Semiann. Prog. Rep. Aug. 31, 1955*, ORNL-1944, p 23.

[5] G. H. Jenks, H. C. Savage *et al.*, *HRP Quar. Prog. Rep. Oct. 31, 1955*, ORNL-2004, p 121, esp. p 131–150.

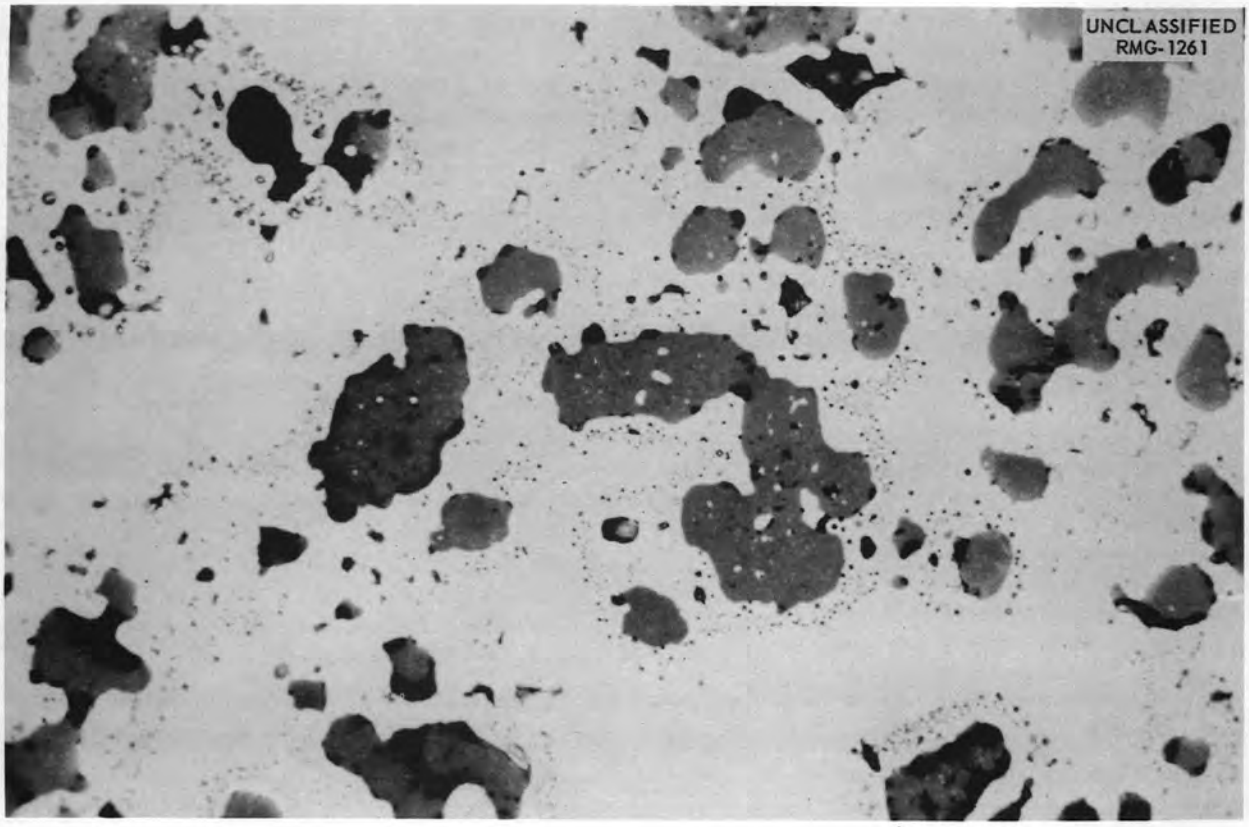

Fig. 45. Sample 19R. Appearance of UO_2 after irradiation. 1000X. (Secret with caption)

[redacted]

tion, HRP in-pile loop L-4-8 was dismantled.[6,7] The operations involved in the dismantling of this loop were more or less the same as those involved in previous loops[4] and were under the supervision of A. R. Olsen, Reactor Experimental Engineering Division.

The first of the vertical dynamic-corrosion loops described previously[8] was disassembled in cell 6 under the direction of C. C. Webster. The operation of this loop in position C-48 of the LITR had to be discontinued after 30 hr due to failure of the pump motor.[9] As a result, the high dose rate and fission-gas activity expected for these loops were not encountered. Disassembly of the loop was completed without difficulty.

Impact and tensile measurements were carried out for ANP, HRP, and WAPD by J. C. Wilson. In the case of the WAPD specimens, the containers were opened in the remote machine shop.[4]

The chemical analyses and uranium-burnup determinations were completed on samples from Pratt & Whitney solid fuel-plate capsules PW-1-12 and PW-1-13, thus concluding ORNL's participation in the Supercritical Water Reactor Experiment.[4] These results are included in a report which is being written at the present time. This report will also include a general summary of the entire experiment.

Final sectioning and metallographic analysis of the first of the MTR-irradiated ANP in-pile loops[10] were performed in the hot cells, as were the post-irradiation testing and metallographic analysis on APPR-type fuel-plate samples irradiated in the MTR. Both these experiments are discussed in greater detail elsewhere in this report.

The new General Mills manipulator was received in September 1955. It was placed into operation after a two-week installation and check-out period. Operation of both General Mills manipulators has become rather dependable and more or less trouble-free. This has been due to several design changes in the manipulators themselves and slight modifications in operating techniques.

A new storage facility was installed in cell 5B. This facility is essentially a manually operated elevator, having a capacity of eight 11-in.-square trays, one above the other. This elevator is completely shielded by 4 in. of lead and lies flush with the cell table when not in use. Storage space is thus provided for a large number of irradiated tensile and impact specimens.

A Voland model 750-D analytical balance was purchased for use in the hot cells and was delivered in October 1955. It has not been installed in the cells, however, pending a modification for density measurements.

Recently correlated data for the calendar year 1955 show that actual experimental operations accounted for 26% of the total hot-cell time available. As indicated in the last progress report, this does not include such operations as installation and testing of experimental equipment, in-cell bench tests, emergency and scheduled maintenance and repairs, removal of material and equipment, and decontamination of the cell.[11] These are all necessary phases of any hot-cell experiment and required 74% of the available cell time. Eventually it is hoped to derive from this cell-use data an approximate figure for the cost of hot-cell time.

With the assistance of the Health Physics Division, careful records were kept of the radiation exposures received by personnel in the Hot Lab Section. Although the exposure in every case was well below accepted ORNL tolerances, all necessary steps are being taken to reduce these exposures still further. Recent additions in manpower and redesign of equipment have already aided this effort. In view of the higher level of activity expected in future experiments, it is imperative that radiation exposures to personnel be kept to an absolute minimum.

---

[6] *Ibid.*, p 121.

[7] H. C. Savage, G. H. Jenks *et al.*, *HRP Quar. Prog. Rep. July 31, 1955*, ORNL-1943, p 105–106.

[8] W. R. Willis, *Solid State Semiann. Prog. Rep. Feb. 28, 1955*, ORNL-1851, p 13.

[9] W. R. Willis *et al.*, *Solid State Semiann. Prog. Rep. Aug. 31, 1955*, ORNL-1944, p 16.

[10] M. J. Feldman *et al.*, *Solid State Semiann. Prog. Rep. Aug. 31, 1955*, ORNL-1944, p 24.

[11] S. E. Dismuke, M. J. Feldman, and E. S. Schwartz, *Solid State Semiann. Prog. Rep. Aug. 31, 1955*, ORNL-1944, p 23.

[redacted]